Palaeogeography, Palaeoclimatology, Palaeoecology 304 (2011) 54–73

Contents lists available at ScienceDirect

Palaeogeography, Palaeoclimatology, Palaeoecology

journal homepage: www.elsevier.com/locate/palaeo

Mudrock sequence stratigraphy: A multi-proxy (sedimentological, paleobiological and geochemical) approach, Devonian Appalachian Basin

Charles A. Ver Straeten [a,*], Carlton E. Brett [b,1], Bradley B. Sageman [c,2]

[a] New York State Museum, The State Education Dept., Albany, NY 12230, United States
[b] Department of Geology, University of Cincinnati, Cincinnati, OH 45221-0013, United States
[c] Department of Earth and Planetary Sciences, Northwestern University, 1850 Campus Drive, Evanston, IL, 60208, United States

ARTICLE INFO

Available online 16 October 2010

Keywords:
Mudrocks
Sequence stratigraphy
Acadian Orogeny
Devonian
Appalachian Basin
Geochemical proxies

ABSTRACT

Delineation of stratigraphic sequences and their component systems tracts in mudrock-dominated facies is generally difficult due to the relatively homogenous, fine-grained nature of the strata. In this study, we apply a multi-proxy analytical approach to a thick Devonian mudrock-dominated succession through detailed analysis of sedimentologic, paleobiologic, and geochemical data through 600 m of mudrock-rich facies. Varied combinations of proxies prove to be most useful in delineating sequence development in anoxic-, dysoxic-, and oxic-dominated mudrock settings, and in mixed mudrock–carbonate and mixed mudrock–sandstone successions. These interpretations are tested against an established sequence stratigraphic framework for 11 Middle to Upper Devonian (mid-Eifelian to lower Famennian) sequences in the Appalachian Basin. The sequences presented here further detail and refine global Devonian T–R cycles Id to IIe of the well known Johnson, Sandberg and Klapper sea-level curve.

The usefulness of proxies in delineating depositional sequences and systems tracts varies dependent on depositional, paleoceanographic, paleoecologic, and early diagenetic conditions. Those proxies that show a range of variations in specific settings, such as grain size, degree of bioturbation, and concentrations of TOC and elements/elemental ratios (e.g., $CaCO_3$, Al, Ti, Mg, Sc, Si, Mo, Ni, V; Si/Al and Ti/Al) may help delineate depositional dynamics related to redox conditions, condensation, dilution, and clastic, biologic, and/or authigenic sediment sources.

In fine-grained, anoxic-dominated facies, interpreted to represent basinal settings, sequences and systems tracts are best delineated by anoxic-related proxies TOC and Mo. In intermediate, dysoxic-dominated settings, TOC, Mo, bioturbation, and Al remain effective indicators of sequence development. In relatively oxygenated, mudrock-rich and carbonate poor sequences, bioturbation may function as the most effective proxy for recognizing systems tracts.

For mixed fine-grained siliciclastic–carbonate successions, concentration and type of $CaCO_3$ (e.g., benthic macroskeletal, pelagic styliolinid/dacryoconarid, and micritic/calcisilt) are useful in identifying position within cycles. In more proximal, carbonate-poor successions, fine- and coarse-grained fractions become increasingly differentiated; these can be distinguished by relatively high Si/Al ratios (Si/Al ≥ ca. 5).

Elemental ratios indicative of coarser clastic input (e.g., Si/Al, Zr/Al and Ti/Al) are applicable to identifying position with a sequence, but they may also be affected by input from eolian, volcanogenic, or biogenic sources. In addition, fluxes of siliciclastic, carbonate, and TOC sediment types may dilute the concentration of the others. Multiple lines of evidence should be examined in interpreting relative depth and position within a sequence.

1. Introduction

Fine-grained siliciclastics, or "mudrocks," comprise a major portion of the sedimentary rock record. Yet, in part due to their fine-grained nature and seemingly homogenous character, mudrock facies and depositional dynamics have received relatively little attention. A combination of new and classical analytical approaches and techniques (e.g., SEM, microfabric studies, petrology and X-ray diffraction (XRD); Schieber, 1999; Schieber and Zimmerle, 1998; Potter et al., 2005) and a greater interest have fueled a rise in mudrock studies (e.g., Potter et al., 1980, 2005; Sageman et al., 2003; Schieber et al., 1998).

The sequence stratigraphic paradigm has revolutionized sedimentary geology since the publication of the seminal work of Vail et al.

* Corresponding author. Tel.: +1 518 486 2004; fax: +1 518 486 2034.
E-mail addresses: cverstra@mail.nysed.gov (C.A. Ver Straeten), brettce@email.uc.edu (C.E. Brett), brad@earth.northwestern.edu (B.B. Sageman).
[1] Tel.: +1 513 556 4556.
[2] Tel.: +1 847 467 2257.

0031-0182/$ – see front matter © 2010 Elsevier B.V. All rights reserved.
doi:10.1016/j.palaeo.2010.10.010

(1977) and associated papers in Payton (1977). Numerous studies discussing the character and development of depositional sequences have fine-tuned the model in a broad range of depositional and tectonic settings (including Catuneanu, 2002; Catuneanu et al., 2009; Miall, 1991; Posamentier and Allen, 1999; Schlager, 1992; Van Wagoner et al., 1990; Wilgus et al., 1988). However, the delineation of depositional sequences and their component systems tracts in mudrock-dominated settings has been relatively neglected, again due to the difficulties of working in relatively homogeneous, fine-grained clastic successions.

A thick succession of Devonian-age marine mudrocks in the northern Appalachian Basin has been the focus of numerous studies since the 1800s, and represents one of the most precisely documented stratigraphic successions in North America. The fine-grained terrigenous facies of the classic Devonian Catskill Delta complex were derived from orogenic highlands developed in New England and adjacent areas. Organic-rich dark shales, of economic significance, constitute a large part of the succession (Roen and Kepferle, 1993).

This study is part of a series of papers examining Middle to Upper Devonian shales from the Appalachian foreland basin using a multi-proxy approach. Work by Murphy et al. (2000a,b,c), Werne et al. (2002), Sageman et al. (2003), and parts of Sageman and Lyons (2003) and Arthur and Sageman (2004), concentrated primarily on depositional processes and organic carbon preservation in black shales of the Union Springs-Oatka Creek, Geneseo, Middlesex, Rhinestreet and Pipe Creek formations. In this paper we apply a multi-proxy analytical approach to the complete succession of Eifelian to Famennian mudrock-dominated facies in two rock cores. The study incorporates detailed sedimentologic, paleobiologic, and geochemical – organic and inorganic carbon, and elemental – analysis to further delineate the stratigraphic sequences and their component systems tracts in fine-grained facies. Various data sets are utilized to characterize the development of mudrock sequences in anoxic-, dysoxic-, and oxic-dominated settings. In addition, we compare our results with the established sequence stratigraphic framework for Middle to Upper Devonian strata in the Appalachian Basin.

1.1. Geologic setting

Devonian mudrocks of the Appalachian Basin were deposited during the latter part of a mid-Paleozoic greenhouse interval (Buggisch, 1991; Isaacson et al., 1997; Ormiston and Oglesby, 1995), in an elongate, east–west oriented retroarc foreland basin situated approximately 30° south of the equator (Joachimski et al., 2009; Scotese and McKerrow, 1990; Witzke, 1990). At times, the basin extended from northern Alabama to Newfoundland in eastern North America.

Appalachian foreland basin sedimentation and kinematics were closely tied to orogenesis, associated with the collision of eastern North America and the Avalonia landmass or a series of terranes (Rast and Skehan, 1993). By the late Early Devonian Emsian age, effects of the Acadian Orogeny migrated from the proximal, ancestral portion of the foreland basin in New England into the main body of what is generally termed the Appalachian Basin. Ettensohn (1985) outlined a model for three to four pulses of Acadian tectonism, separated by intervals of relative quiescence, Acadian Tectophases I–IV, based on Lower Devonian to Lower Mississippian sedimentation trends.

Middle to Upper Devonian strata in western New York are part of the Catskill Delta Complex, an eastwardly thickening wedge of dominantly terrigenous-derived marine to terrestrial sediments (Friedman and Johnson, 1966; Woodrow and Sevon, 1985). During the middle Eifelian to lower Frasnian, western New York lay on the margin of the western, craton-ward ramp of the foreland basin system. Due to a westward shift of the basin through time, middle Frasnian to lower Famennian strata were deposited in the central trough of the basin.

Mudrocks included in this study (Fig. 1) comprise strata of the Eifelian, Givetian, Frasnian, and basal Famennian stages, and represent approximately 15 m.y. (Kaufmann, 2006). The interval spans 25 conodont zones (see Kaufmann, 2006 for summary) and 24 to 25 goniatite zones (House, 1978; House and Kirchgasser, 1993, 2008).

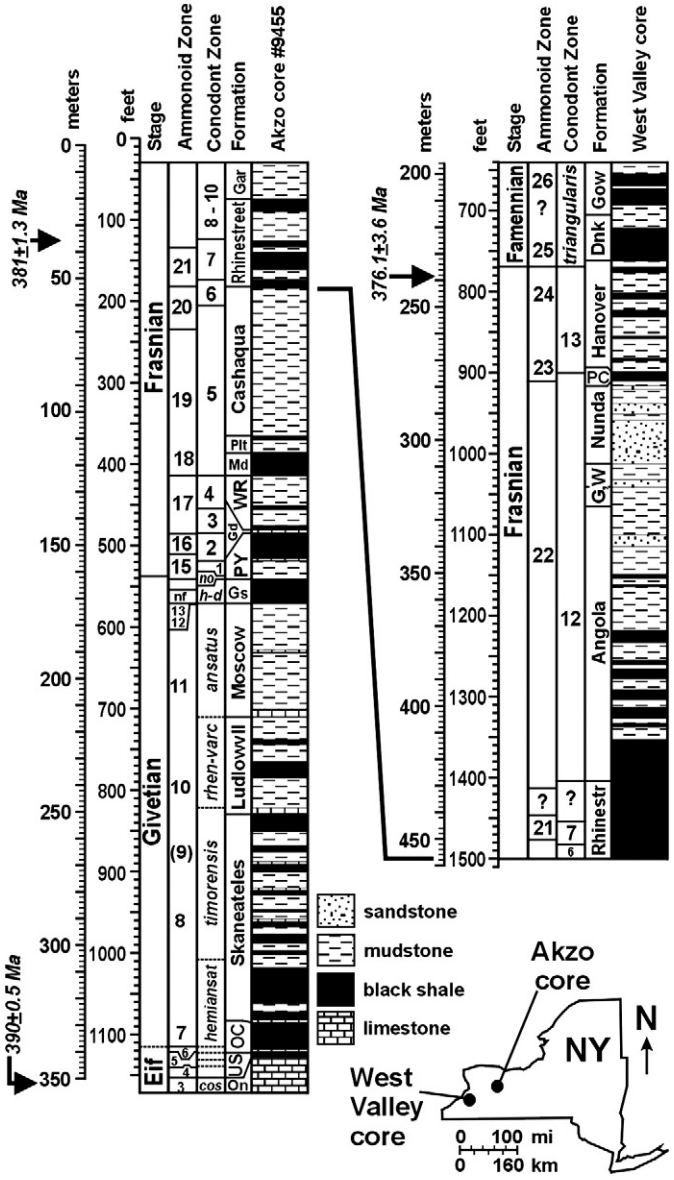

Fig. 1. Stratigraphy and localities of Devonian shales in the Akzo #9455 and West Valley cores, western New York State. Geochronologic dates from Tucker et al. (1998) and Kaufmann (2006). Formation/member name abbreviations (in vertical order) are On = Onondaga; US = Union Springs; TOC = Oatka Creek; Ludlowvll = Ludlowville; Gs = Geneseo; PY = Penn Yan; Gd = Genundewa; WR = West River; Md = Middlesex; Plt = Pultney; Rhinestr = Rhinestreet; Gar = Gardeau; G,W = Gardeau and West Hill; PC = Pipe Creek; Dnk = Dunkirk; Gow = Gowanda. Other abbreviations are Eif = Eifelian; nf = no fauna found; *cos* = *costatus*; *hemiansat* = *hemiansatus*; *rhen-varc* = *rhenanus-varcus*; *h-d* = *hermanni-disparilus*. Unlabeled conodont zones above *cos* = *australis*, *kockelianus*, *eiflius*, and *ensensis*, in vertical order. Conodont data from Klapper (1971, 1981, 1989), Kirchgasser et al. (1994), Klapper et al. (1995), D.J. Over and W.T. Kirchgasser (pers. commun.), and Brett (unpublished data). Goniatite data after House (1978) and House and Kirchgasser (1993).

The strata, with the topmost Onondaga Formation at the base, are subdivided into 22 formations assigned to five groups, in ascending order, the Hamilton, Genesee, Sonyea, and West Falls groups, and lower part of the Canadaway Group); (see Fig. 1; Rickard, 1975). The succession represents one of the most complete and thoroughly studied Devonian successions in North America, and is recognized as the North American standard section for the Devonian (Baird et al., 2000; Brett and Baird, 1986, 1990, 1994, 1996; Brett et al., 1990;

Colton and de Witt, 1958; de Witt and Colton, 1959, 1978; Gray, 1991; House and Kirchgasser, 1993; Kirchgasser et al., 1989, 1994; Mayer, 1994; Mayer et al., 1994; McCollum, 1991; Miller, 1991; Pepper and de Witt, 1950; Pepper et al., 1956; Ver Straeten, 1996, 2007; Ver Straeten et al., 1994, research notes; C.E. Brett, G.C. Baird, D.J. Over, and W.T. Kirchgasser, pers. commun.).

1.2. Sequence stratigraphy

1.2.1. Overview

Sequence stratigraphy is a powerful tool analyzing time–rock relationships (Catuneanu, 2002; Catuneanu et al., 2009; Coe, 2003; Emery and Myers, 1996; Posamentier and Allen, 1999; Van Wagoner et al., 1988; Wilgus et al., 1988). It allows chronostratigraphic division of the rock record into cyclic, unconformity-bound, genetically related successions of strata (Van Wagoner et al., 1988). A 'depositional sequence' is the fundamental, meso-scale unit of sequence stratigraphy.

Following on the early development of the sequence stratigraphic paradigm, the model has been fine-tuned, and is broadly applicable through and across marine and terrestrial facies. The delineation of depositional sequences and component systems tracts is based on the recognition of numerous sedimentologic and paleontologic factors that include: unconformities, lithofacies trends, distinctive sedimentologic and paleoecologic shifts, condensed intervals, trace fossils and ichnofabric, as well as biostratigraphic and taphonomic trends (e.g., papers in Brett, 1995, 1998; Emery and Myers, 1996; Ghibaudo et al., 1996; Posamentier and Allen, 1999; Savrda, 1991; Van Wagoner et al., 1990; Wilgus et al., 1988).

Major, minor, and trace element geochemistry has received less attention in sequence stratigraphic studies. When utilized in the past, it was often focused on metals that are enriched under redox conditions, in organic-rich, fine-grained facies (Sethi and Leithold, 1997). More recent studies integrate a broader suite of elements and elemental ratios, to examine mudrock deposition (Algeo et al., 2004; Jaminski et al., 1998; Sageman and Lyons, 2003; Sageman et al., 2003). Many processes may affect the elemental record of mudrocks, including sediment input source, solubility, provenance, weathering, transport and hydrodynamic sorting/grain size, oxygen availability, biogenic effects, diagenesis, and metamorphism (Spencer et al., 1967; Wintsch and Kvale, 1994; Young and Nesbitt, 1998). In addition, some elements may have multiple sources and potential transport paths, for example quartz can be of terrigenous detrital, volcanic, biogenic, and diagenetic origin and enter the system from riverine, eolian, ashfall/flow, and pelagic rain (Sageman and Lyons, 2003; Sageman et al., 2003). Integration of elemental data with other analytical approaches, such as X-ray diffraction, thin section petrology, and statistical analysis as well as an understanding of processes acting within the depositional system permit the utilization of elemental data in sequence analysis.

The elemental geochemistry of fine-grained rocks is generally thought to be little altered by diagenesis, even in metamorphic facies (Shaw, 1954; Spencer et al., 1967; Wintsch and Kvale, 1994). However, as noted by Bloch (1998), the mobilities of various elements are variable; some appear to be relatively immobile (Ti and Al), whereas others may be exported (Si) or imported (Fe, Mg and K) to or from shales.

Due to the problems of their fine-grained and often homogeneous nature, the depositional dynamics and the development of depositional sequences in clastic mudrocks have generally received less attention, or have focused on specific fine-grained intervals or facies within systems tracts (e.g., condensed shales/transgressive shales). Studies of sequence development in mudrock-dominated settings and organic-rich facies include Hallam and Bradshaw (1979), Wignall (1991a,b), Curiale et al. (1991), Pasley et al. (1991), Schwalbach and Bohacs (1992), Creaney and Passey (1993), Katz and Pratt (1993), Wignall and Maynard (1993), Macquaker and Taylor (1996), Mann and Stein (1997), Bohacs (1998), Schutter (1998), Macquaker et al. (1998), Schieber (1998), Williams et al. (2001), and Algeo et al. (2004).

1.2.2. Devonian sequence stratigraphy and sea level curves

The Taghanic Unconformity splits the Devonian succession examined here into the early and late stages of Sloss's (1963) Kaskaskia Supersequence. At least 11 significant ("third order") depositional cycles characterize middle Eifelian to lower Famennian strata of the study interval. The lower five have been discussed within a sequence stratigraphic framework (Brett and Baird, 1994, 1996; Brett and Ver Straeten, 1994, 1997; Ver Straeten, 2007; Ver Straeten and Brett, 1995); upper cycles/sequences are outlined by House and Kirchgasser (1993), Filer (1994) and Over et al. (2001). Most of the third order sequences correspond to Devonian transgressive–regressive (T–R) cycles Id–IIe of Johnson et al. (1985, 1995; however, see modifications of Brett et al., 1997, 2011–this issue) which, owing to their widespread recognition across Europe, North Africa, and North America, are attributed to changes in eustatic sea level. Several smaller scales of cyclicity are also recognized. The entire succession is superposed over two tectonic cycles (Acadian Tectophases II and III of Ettensohn, 1985).

2. Material and methods

Two cores, the Akzo core #9455 and Western New York Nuclear Fuel Service core #1 = "West Valley" core, middle Eifelian to Lower Famennian (Fig. 1), were obtained for analysis from the distal foreland basin succession. The cores were chosen for their relative completeness, predominantly mudrock composition, overlap of strata between the two cores, and a relatively low degree of thermal alteration, significant to the analyses of TOC and stable isotopes of carbon. The geographic position of the cores lies within a band between illite crystallinity isograds of 0.10 to 0.11, which corresponds to conodont alteration index (CAI) values of approximately 1.5 to 2, and diagenetic temperatures in the range of approximately 50° to <200 °C (Hosterman, 1993; Hosterman and Whitlow, 1983).

The stratigraphically lower "Akzo" core is 330 m-thick, and spans the mid Eifelian to mid Frasnian age. It was obtained from the Akzo-Nobel Salt Corporation, Livingston County, NY. The 260 m-thick upper ("West Valley") core, drilled by Western New York Nuclear Fuel Service in Cattaraugus Co., NY, and reposited at the New York State Museum/Geological Survey, spans the mid Frasnian to lower Famennian stages. The two cores overlap in strata of the middle Frasnian Rhinestreet Formation. Both cores were described at mm- to cm-scale for physical and paleobiological characters (e.g., lithology, sedimentary structures, sedimentary fabric/bioturbation/ichnofabric, color, carbonate type, burrow-type/ichno- and macrofauna). The degree of bioturbation was recorded on a seven point scale — well to moderately to poorly laminated; burrowed; and poorly to moderately to highly bioturbated, 1–7, respectively. Rock color was interpreted from the core face or fresh surfaces based on comparison with the Rock Color Chart of Goddard et al. (1948). Carbonate type (by %) was divided into: 1) macrofaunal skeletal material; 2) styliolinids, mm length, elongate, conical shells of Devonian age interpreted to be of pelagic habit; and 3) micrite/calcisilt, based on visual observation of the cut core surface. Macro- and ichnofauna data were recorded to the lowest determinable taxonomic level. The cores were correlated with local outcrops at bed-scale where possible, within the high resolution, local to regional stratigraphic framework of the New York Devonian (see references mentioned previously).

Core samples for geochemical analyses were collected and crushed at 60 or 120 cm intervals through the cores, except key intervals that were analyzed every 15–20 cm. Powdered samples were processed and analyzed for $\delta^{13}C_{org}$, total and inorganic carbon, and major, minor, and trace elements. Weight% total carbon and inorganic carbon were determined by coulometry (Engleman et al.,

1985; ±1.0% errors) on a UIC Carbon Coulometer. Total organic carbon (TOC) values were determined by subtraction of inorganic carbon (IC) from total carbon (TC). Concentrations of 32 major, minor, and trace elements, that include Be, Na, Mg, Al, Si, P, K, Ca, Sc, Ti, V, Cr, Mn, Fe, Co, Ni, Cu, Zn, Sr, Y, Zr, Mo, Ba, La, and Pb were determined by inductively coupled plasma emission mass spectrometry (Lichte et al., 1987; XRAL Laboratories, multi-acid and aqua regia (Si) digestion techniques).

X-ray diffraction and thin section petrologic analyses were performed on a select set of 28 samples to "ground truth" mineralogical interpretations of the elemental data. XRD was performed at Northwestern University [Rigaku diffractometer, set at 35 kV/15 mA, using copper (CuK_a) radiation]. Thin section petrologic analysis was performed on the same samples. Additional mineralogical information was obtained from Hosterman and Whitlow (1981, 1983) and from a core (Stewart 6701 core, Livingston Co., NY) proximate to Akzo core #9455 of this study.

Q-mode factor analysis was applied to the Akzo and West Valley data sets to better delineate the relationships between the accumulated data, and for the purpose of more closely delineating sedimentary trends and processes. Selected sets of 26 and 28 variables for TOC; ± degree of bioturbation, $\delta^{13}C_{org}$; and the elements listed above at evenly distributed (ca. 1.2 m) intervals were subjected to statistical analysis for each core and various subsets of the data. Q-mode analyses were performed, data normalized to highest value for each variable, using Cabfac for Macintosh, employing a cos-theta measure of similarity. Varimax rotations were applied to Q-mode results and several factor curves were generated for each data set.

3. Results

3.1. Introduction

In order to utilize various sedimentologic, paleobiologic, and geochemical proxies in the delineation of mudrock-dominated sequences, we initially characterized proxy trends through three well-defined sequences, representing anoxic, dysoxic, and oxic settings. For this purpose we chose three sequences within the Middle Devonian Hamilton Group which have been extensively studied, and have well-established sequence stratigraphic frameworks (Brett and Baird, 1994, 1996; Brett and Ver Straeten, 1997; Ver Straeten, 2007; Ver Straeten and Brett, 1995).

In this paper, depositional sequences are subdivided into transgressive, highstand, and late highstand systems tracts (TST, EHST and LHST, respectively). TSTs represent transgressive facies, beginning with initial facies patterns indicative of deepening upward; they may overlie a sequence-bounding unconformity. TSTs are bounded at the top by a maximum flooding surface, representative of the maximum landward point of the shoreline within a sequence. EHSTs overlie the surface of maximum flooding, and are characterized by aggradational facies patterns. A late highstand systems tract (LHST) is characterized by generally shallowing facies patterns, formed during a sea level fall, or forced regression; we favor the term late highstand for third-order sequences because it is regressive in average behavior but with some deepenings at the scale of smaller sequences, in contrast to distinctly progradational FSSTs seen in some fourth-order sequences. A lowstand systems tract (LST) may be found at the base of a sequence. These progradational packages form during the initiation of base level rise, when sedimentation rate is greater than the accommodation space created by the rise. LSTs are only recognized in some sequences and certain geographic positions in the basin, and are interpreted as missing at a sequence bounding unconformity in others. For further information, see Wilgus et al. (1988), Emery and Myers (1996), Posamentier and Allen (1999), Catuneanu (2002), and Coe (2003).

3.2. Anoxic-dominated Sequence 2: the Oatka Creek Formation

Sequence 2 of this study comprises strata of the Oatka Creek Formation, in the lower part of the Middle Devonian Hamilton Group. The succession is dominated by black shales, with two thin limestones at the base, the Hurley and Cherry Valley members, and one fossiliferous limestone bed low in the formation (Fig. 2). A relative sea level curve and associated sequence stratigraphic interpretation for the interval is adapted from Ver Straeten (2007; modified from Brett and Baird, 1996; Ver Straeten and Brett, 1995). Plotted against this framework are degree of bioturbation, weight% TOC and $CaCO_3$, %

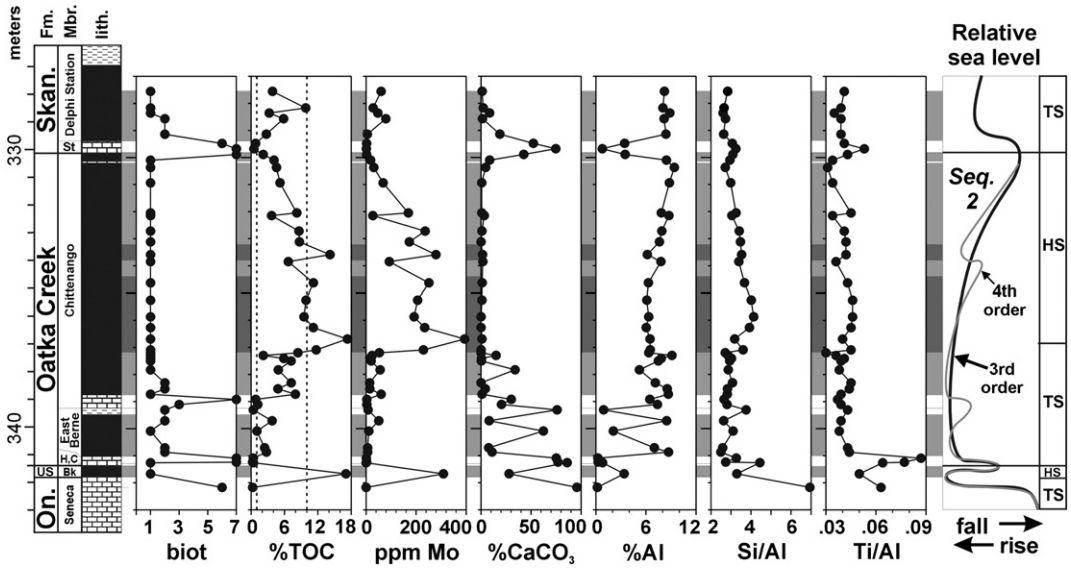

Fig. 2. Stratigraphy and proxy trends for depositional Sequence 2 (Oatka Creek Fm.). Bioturbation ("biot") measured on rank scale, where 1 = fully laminated fabric, 7 = fully bioturbated fabric, and 0 = no fabric visible. LS = lowstand systems tract; TS = transgressive systems tract; HS = highstand systems tract. Relative sea level curve (3rd order) and sequence stratigraphy modified after Ver Straeten (2007). Abbreviations: Bk = Bakoven; Fm. = Formation; H,C = Hurley and Cherry Valley members; lith. = lithology On = Onondaga; Skan = Skaneateles; St = Stafford; US = Union Springs. Light gray bands behind data columns = TOC between1 and 10%; Dark gray bands = TOC ≥ 10%.

carbonate type, concentrations of Al, Si, and Mo, and the ratio of Si/Al and Zr/Al for Sequence 2. A more detailed analysis of proxy trends through Sequence 2 has been presented by Werne et al. (2002).

The basal Sequence 2 boundary is unconformable in outcrops and other cores in the vicinity of the Akzo core (Ver Straeten et al., 1994; unpublished data C.A. Ver Straeten), and cuts downward toward the craton into the LHST–EHST to TST of underlying Sequence 1. Proxies in Fig. 2 show initial high values for $CaCO_3$ and bioturbation, with corresponding low values of other proxies. These trends are succeeded by an interval of widely fluctuating variations in all proxies. The interval does show overall declines, however, in $CaCO_3$ and the degree of bioturbation and a general rise in TOC. Beds low in carbonate content show relatively high concentrations of detrital indicators (e.g., Al and Si). A thin fossiliferous bed, indicated in the stratigraphic column, represents the base of the TST of a second prominent fourth-order subsequence.

A peak in detrital content at approximately 338 m depth in the Akzo core is succeeded by a sharp change in the shales. An abrupt rise in the concentration of TOC (>17%) and the redox indicator Mo (ca. 400 ppm) is coincident with a decline in both carbonate content (to zero) and detrital proxies, and a shift to fully laminated textures (bioturbation = 1).

In overlying strata $CaCO_3$ remains at zero, sedimentary fabric is fully laminated throughout, and detrital indicators are relatively stable. TOC is also relatively stable and then declines to approximately 334 m, coincident with a rise in Al, Si, and related ratios. Another sharp, if less significant, rise in TOC, correlated with a drop in detrital proxies, is followed by a general decline in TOC concentration and a rise in detrital indicators upward to the base of Sequence 3.

3.3. Dysoxic-dominated Sequence 3: the Skaneateles Formation

The stratigraphic framework of black shales, dark gray mudstones, and marlstones to limestones of the Skaneateles Formation and lower part of the Ludlowville Formation in the middle part of the Hamilton Group represents the TST, EHST, and LHST of Sequence 3 and overlying parts of the TST and lower EHST of Sequence 4 (Fig. 3). Relative sea level curves modified after Brett and Baird (1996) indicate that three subsequence-scale cycles are superimposed on Sequence 3.

Deposition above the basal limestone of Sequence 3 can be subdivided into five phases, the first (329–309 m) characterized by fluctuating concentrations of TOC, carbonate, and detrital input, with a general rise of TOC versus decline of the latter two, respectively. The following phases of deposition are discernable: A) an initial interval marked by stable, low detrital/high carbonate values (309–299 m); B) rhythmically alternating carbonate and detrital values (299–267 m); C) relatively stable high detrital/low carbonate values (267–258 m); and D) a decline in terrigenous clastic values, accompanied by an increase in $CaCO_3$ and TOC (258–251 m). The degree of bioturbation exhibits three cycles of rise and decline above the sequence base. TOC shows an initial rise above the basal limestone (ca. 9%), an overall decline through the first phase of deposition, and then rhythmic fluctuations around 1% through the remainder of Sequence 3. Background levels for the associated redox proxy Mo through the sequence are close to zero, except for intervals that are relatively enriched in TOC. Carbonate type through the sequence is initially dominated by calcisilt/micrite, but progresses upward through styliolinid-rich to more calcisilt/micrite facies to macrofossil type limestones leading into a coral–bryozoan–brachiopod rich association in the basal carbonate of Sequence 4.

3.4. Oxic-dominated Sequence 5: the Moscow Formation

The upper part of the Hamilton Group succession is characterized by fossiliferous, gray mudrock-dominated facies of the Moscow Formation (Fig. 4). It is separated from overlying black shales and minor limestones of the Geneseo Formation in the Akzo core by the Taghanic Unconformity. Interpreted relative sea level curves and sequence stratigraphy for Sequence 5 are modified after Brett and Baird (1996).

TOC values in Sequence 5 are significantly depressed relative to Sequences 2 and 3, and $CaCO_3$ is also less compared to Sequence 3. The concentration of TOC maintains a narrow linear range of approximately 0.3 to 0.5 wt.% above the sequence bounding TST limestones. $CaCO_3$ shows a general decreasing trend above the basal TST limestones to a position in the middle HST (ca. 187 m), then rises again before another significant drop in the uppermost Moscow beds. This succession may mark the lower part of another, previously unrecognized sequence in the upper Moscow Formation, identified by

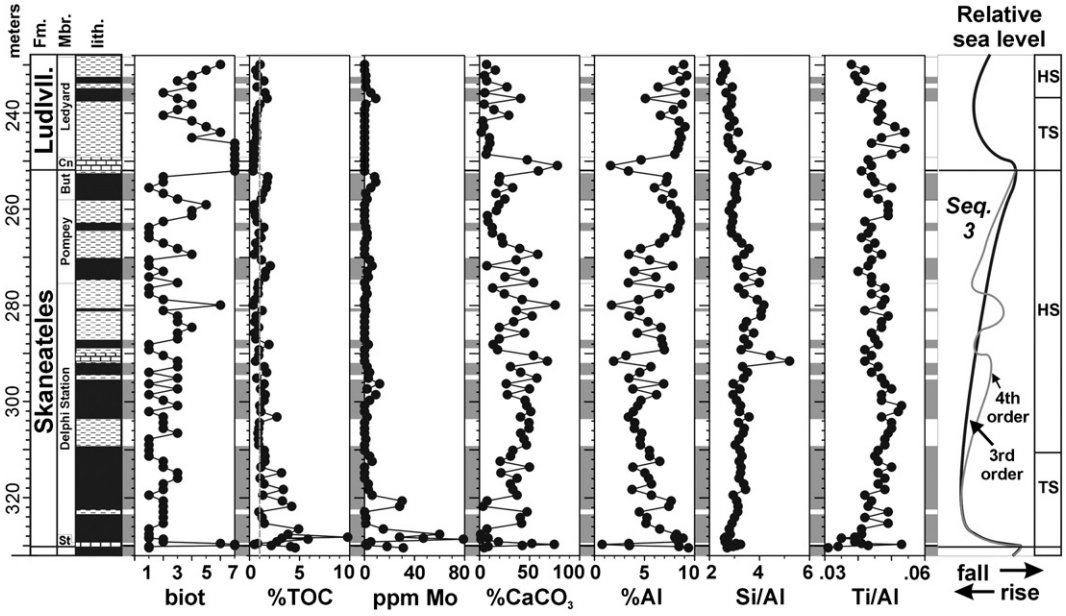

Fig. 3. Stratigraphy and proxy trends for depositional Sequence 3 (Skaneateles Fm.). Relative sea level curve (3rd order) and sequence stratigraphy modified after Brett and Baird (1996). Abbreviations: But = Butternut; Cn = Centerfield; Ludlvll. = Ludlowville; St = Stafford. Light gray bands behind data columns = TOC>1%.

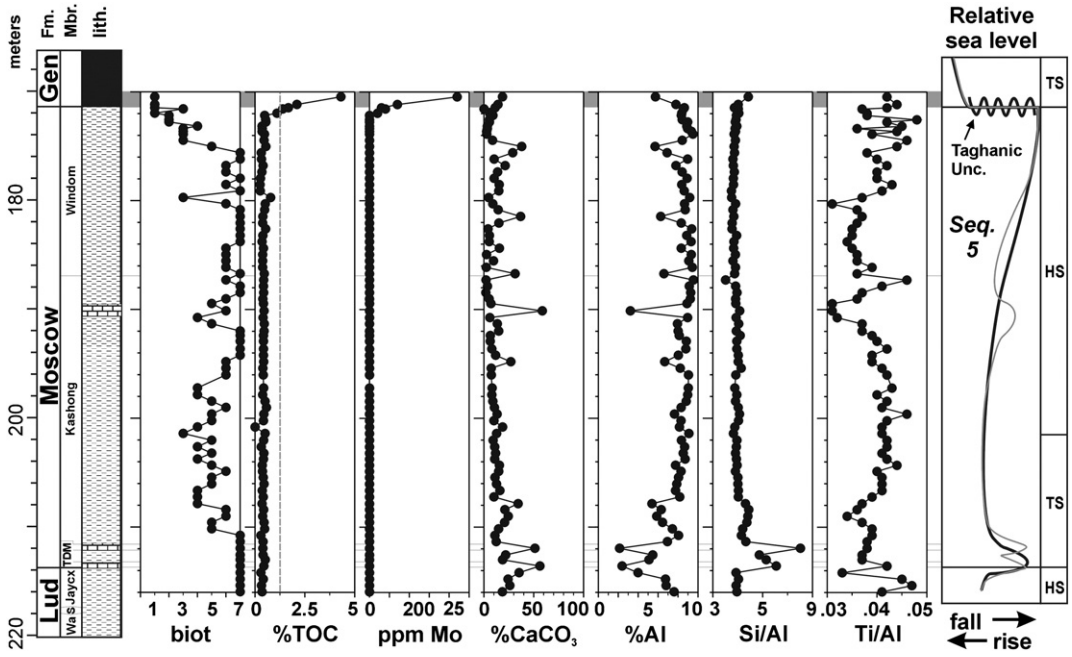

Fig. 4. Stratigraphy and proxy trends for depositional Sequence 5 (Moscow Fm.). Taghanic Unconformity at base of Sequence 6 is position of missing Tully Limestone (= LST and early TST). Relative sea level curve (3rd order) and sequence stratigraphy modified after Brett and Baird (1996). Abbreviations: Jaycx = Jaycox; Lud = Ludlowville; Gen = Geneseo; S = Spafford; TDM = Tichenor, Deep Run and Menteth members, low to high; Wa = Wanakah. Light gray bands behind data columns = TOC>1%.

Brett et al. (2011–this issue). Bioturbation is not linked as closely to $CaCO_3$ content as in Sequences 2 and 3 (e.g., minimal bioturbation at ca. 200 m versus minimal carbonate at 187 m), but they do, in general, maintain a co-varying relationship. Notable is the dominance of macroskeletal carbonate and the high degree of bioturbation throughout Sequence 5, indicative of well-oxygenated, ecologically diverse, relatively shallow shelfal environments.

Elemental detrital proxies in Sequence 5 are consistent with the previous sequences. A secular increase in most detrital components (Al and Si) occurs from uppermost TST through the HST within the Moscow Formation. A Si/Al spike low in the TST occurs within thin, silt- to sand-rich, calcareous mudstones of the Deep Run Member, situated between the pair of basal TST limestone beds. Distinct negative spikes in detrital indicators are, as previously noted, directly related to positive carbonate peaks. Increased concentrations of TOC and clastic-related proxies in the LHST, below the Taghanic Unconformity, also correspond to a decrease in $CaCO_3$ of macroskeletal type and bioturbation. In outcrop this event is represented by a dark gray, sparingly fossiliferous mudstone to shale of the Gage Gully beds of Brett and Baird (1994). This anomalous increase in TOC in the LHST is analogous to TOC enrichment in the same position within Sequence 3; and as in that case, is interpreted here to represent part of a 4th order cycle within Sequence 5. However, as noted, Brett et al. (2011–this issue) propose that this may represent the lower part of another third-order sequence. All physical, biological, and geochemical proxies undergo major alteration across the Taghanic Unconformity into the Geneseo Shale, in the overlying sequence.

3.5. Trends through the Akzo and West Valley cores

Two larger-scale cycles, associated with phases of active tectonism to quiescence, Acadian Tectophases II and part of III of Ettensohn (1985), are visible in the large scale proxy trends of bioturbation, TOC, Mo, and the detrital-related proxies Al and Si in the Akzo and West Valley cores (Figs. 5 and 6). The first tectonic cycle comprises strata of the Union Springs to Moscow formations to the Tully Formation, the latter of which is absent at the Taghanic Unconformity, at 171.5 m in the Akzo core. Thin, relatively condensed strata with high TOC/Mo concentrations and laminated fabrics in lower Hamilton strata (Sequences 1 and 2) give way upward to thicker, highly bioturbated strata and organic-poor strata with low redox-related signals, accompanied by relatively high concentrations of detrital-related proxies. Carbonate shows initial low concentrations, punctuated by sharp peaks, followed by a general rise (into Sequence 3, Skaneateles Fm.), and then by a decline correlatable with the rise in detrital proxies.

Proxy trends through strata above the Taghanic Unconformity, in general, mirror lower Hamilton trends of high TOC and redox signatures as well as low bioturbation, with the exception of the decline of carbonate in the mudrock system. Cyclic, medial-scale alternations of apparent anoxic to dysoxic facies (e.g., Sequences 2 and 3) characterize the succession through the Akzo core upward into the middle of the West Valley core succession, where trends in TOC/redox and bioturbation reflect more oxic conditions. Carbonate levels decrease to near zero levels and overall clastic concentration achieves its highest levels, to the degree, in fact, that high % Si and a Si/Al ratio >5 indicate a temporary shift from mudrock- to sand-dominated facies in the Nunda Formation. Laminated fabrics through the sandstones of the Nunda are seen in core to be associated with relatively thick beds representative of episodic turbidite or tempestite deposition. Overlying the Nunda Formation, proxies generally again mimic trends within Sequences 2 and 3, with a few signals analogous to oxic conditions in Sequence 5. At smaller scales, trends for proxies through the Akzo and West Valley cores in most intervals show additional higher-scale fluctuations.

4. Interpretations

4.1. Factor analysis and mudrock systems interpretation

Statistical Q-mode factor analysis was applied to the quantitative geochemical data sets and subsets from the Akzo and West Valley cores. Loading of analyzed variables, including concentrations of TOC and the elements Be, Na, Mg, Al, Si, P, K, Ca, Sc, Ti, V, Cr, Mn, Fe, Co, Ni, Cu, Zn, Sr, Y, Zr, Mo, Ba, La, and Pb outline separate factors for detrital input, carbonate input, and an organic carbon/redox association in the

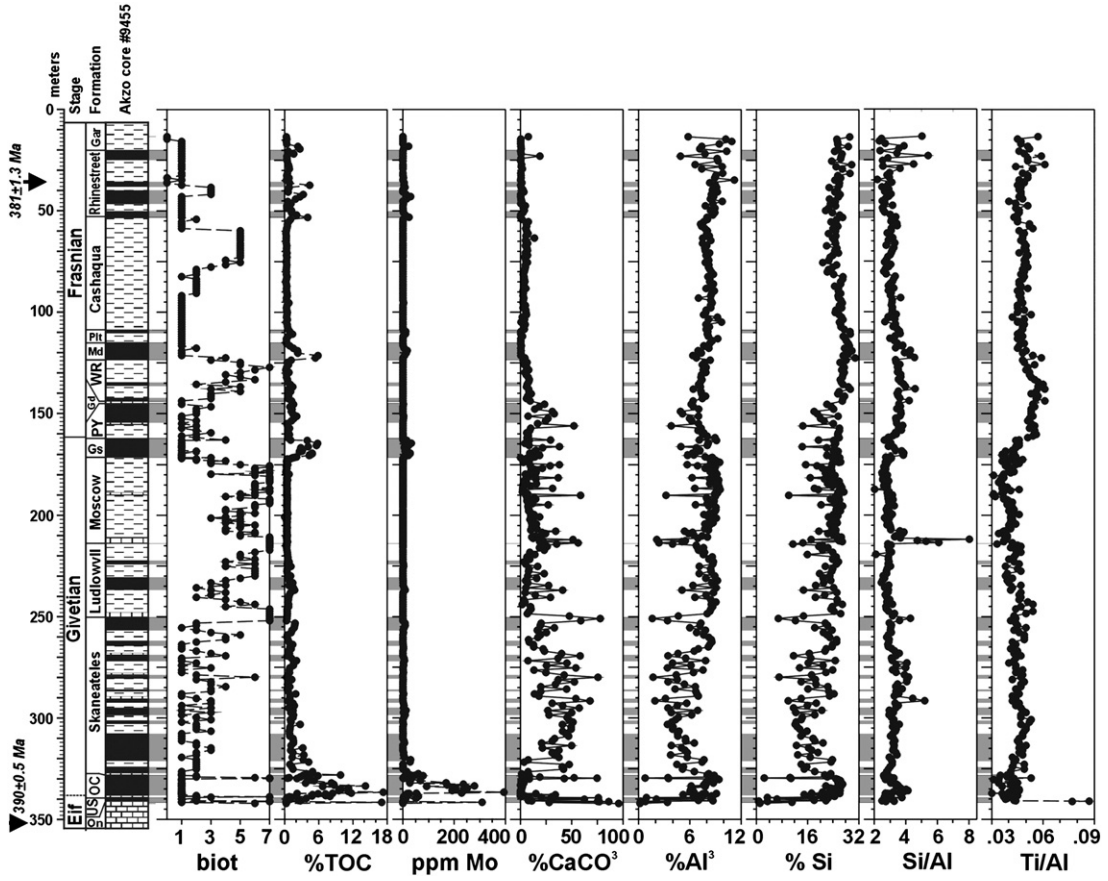

Fig. 5. Stratigraphy and proxy trends for Eifelian to Frasnian strata of Akzo core #9455. Abbreviations as in Fig. 1. Relative sea level curves are shown in Fig. 7.

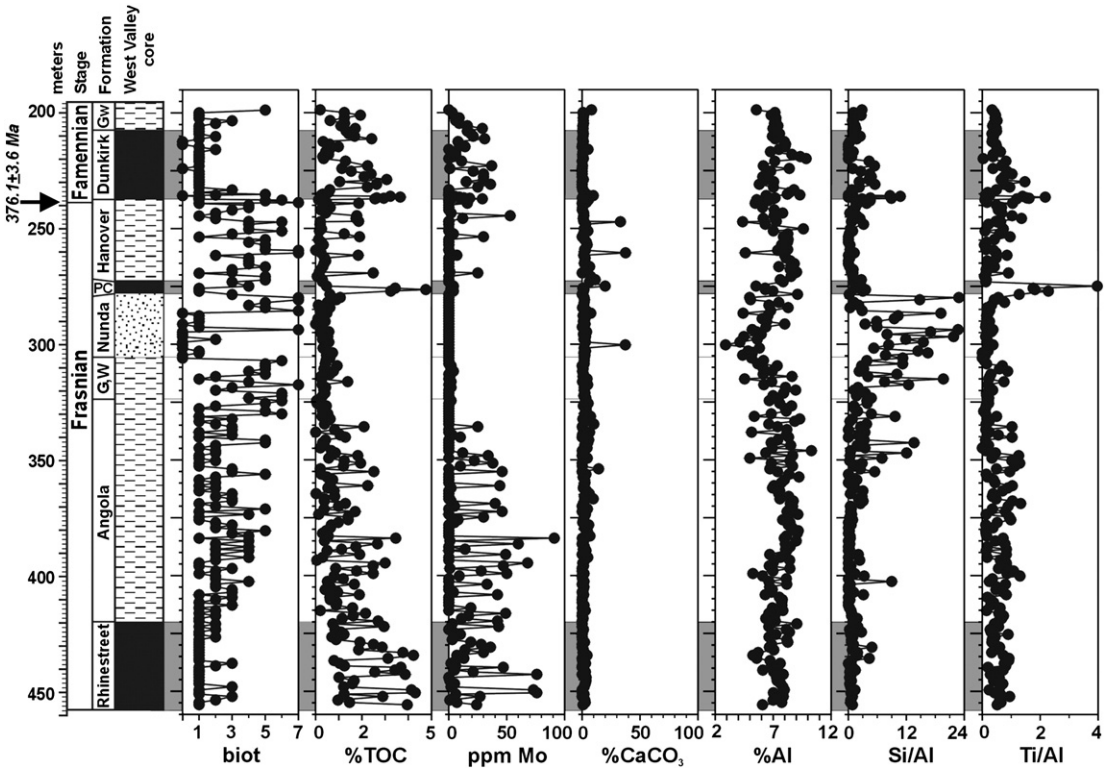

Fig. 6. Stratigraphy and proxy trends for Frasnian to Famennian strata of the West Valley core. Abbreviations as in Fig. 1. Relative sea level curves are shown in Fig. 7.

Akzo and West Valley cores. Applying a range of two to ten factors to complete core data sets, it was found that three factors best explain most of the variation in the data of both cores; these represent loadings that reflect detrital input, TOC/redox-related elements, and carbonate. Other factors were relatively minor and their significance was generally unclear (Tables 1–3).

Factor analysis performed on data from the Akzo core (Table 1) indicates that three main factors account for 96% of the variation through the whole core. The first of these exhibits positive loadings on elements associated with detrital input into the depositional system (e.g., Na, Zr, Ti, Si, Al, and K) and a negative Ca loading. A strong Ca loading on the second factor, associated with weak Mn, Y, and Mg, point to an association with carbonate. Factor 3, with a strong Pb loading and weaker associations with TOC, Mo, Ni, and Co, is tied to redox-related conditions during deposition of the strata. A fourth, relatively weak factor, that explains only 2% of the variation in the Akzo data set, is associated with positive loadings of Pb, Ba, La, and especially Na, and weak negative loadings of Cr, Sc, K and Mg. It may be attributable to detrital clays with or without the sand-sized fraction.

Variations in the complete West Valley data set (Table 2) are best explained by four factors (= 98% of variation). Factors 1 and 2 represent TOC/redox loadings; the second one is also associated with a negative loading on fine-grained clastics in the system (K, Sc, Al, Ti, and others). Factor 3 shows a moderate loading on the coarse-grained components of the system (represented by Si, Zr, and Ti and others). Factor 4 is attributable to carbonate (Ca, Mn, Y, and Sr).

Three factors in the second West Valley data set (Table 3, "no sandstone" samples only) explain 97% of the variation (37%, 32%, and 23%, respectively). The first factor is associated with the fine-grained detrital component of the system (weak Sr, Sc, Al, K and Ti) and a negative organic carbon/redox signal (low TOC; weak Mo, Ni and Pb).

Table 2
Q-mode factor analysis, WV core (sorted; all samples).

Var.	Factor 1	Var.	Factor 2	Var.	Factor 3	Var.	Factor 4
TOC	**0.50**	**TOC**	**0.40**	**Si**	**0.59**	**Ca**	**0.51**
Mo	**0.37**	**Mo**	**0.26**	**Zr**	**0.44**	**Mn**	**0.47**
Ni	**0.36**	Pb	0.17	**P**	**0.35**	**Y**	**0.34**
Pb	**0.30**	Co	0.11	**Co**	**0.31**	**Sr**	**0.28**
Na	**0.27**	Si	0.10	**Ti**	**0.22**	**Pb**	**0.23**
K	**0.21**	Ca	0.06	Y	0.19	Fe	0.17
V	**0.20**	Zn	0.05	Ba	0.16	Sc	0.16
Be	**0.20**	Ni	0.04	Na	0.15	P	0.15
Ba	0.16	Zr	0.02	Mg	0.09	Mg	0.14
Ti	0.14	Cu	0.01	La	0.09	Ni	0.12
Cr	0.13	P	0.00	Mn	0.07	TOC	0.12
Si	0.13	Mn	−0.02	Fe	0.07	Cr	0.11
La	0.13	Y	−0.02	Al	0.01	Zn	0.08
Al	0.13	Na	−0.06	Sr	0.01	Al	0.05
Sc	0.11	Fe	−0.10	Ca	−0.01	Cu	0.03
Zr	0.10	Cr	−0.14	Zn	−0.02	Be	0.02
Fe	0.09	V	−0.16	Sc	−0.02	Co	0.02
Cu	0.07	La	−0.18	Cu	−0.02	Mo	0.01
Mg	0.07	**Ti**	**−0.20**	TOC	−0.05	K	−0.01
Co	0.05	**Ba**	**−0.20**	Be	−0.05	Si	−0.01
Zn	0.05	**Mg**	**−0.24**	Mo	−0.08	La	−0.02
Y	0.01	**Sr**	**−0.29**	Cr	−0.08	Zr	−0.03
Sr	0.00	**Al**	**−0.29**	Pb	−0.13	V	−0.05
P	−0.09	**Be**	**−0.30**	V	−0.14	Ti	−0.11
Ca	−0.10	**Sc**	**−0.30**	Ni	−0.14	Na	−0.19
Mn	−0.14	**K**	**−0.36**	K	−0.14	**Ba**	**−0.26**
Sum[1]	37.38		31.76		23.23		5.77
Sum[2]	37.38		69.14		92.37		98.15

Factor 1 = TOC/redox.
Factor 2 = TOC, Mo; − fine detrital (shale).
Factor 3 = coarse detrital (sandstone).
Factor 4 = carbonate.

Table 1
Q-mode factor analysis, Akzo core (sorted).

Var.	Factor 1	Var.	Factor 2	Var.	Factor 3	Var.	Factor 4
Na	**0.33**	**Ca**	**0.77**	**Pb**	**0.61**	**Na**	**0.51**
Ba	**0.32**	**Y**	**0.37**	**TOC**	**0.35**	**Pb**	**0.30**
Zr	**0.32**	**Mn**	**0.32**	**Ni**	**0.25**	**Ba**	**0.28**
Ti	**0.32**	**Mg**	**0.26**	**Mo**	**0.25**	**La**	**0.27**
Si	**0.28**	Sr	0.17	**Co**	**0.25**	P	0.15
La	**0.28**	P	0.13	**Fe**	**0.23**	Zr	0.13
Al	**0.27**	Si	0.13	**Be**	**0.20**	Mn	0.11
K	**0.24**	La	0.12	V	0.18	Ca	0.08
Mg	**0.24**	Sc	0.10	Cu	0.15	Fe	0.06
Sc	**0.22**	K	0.06	Y	0.15	Y	0.03
Fe	0.19	Fe	0.06	Cr	0.12	Zn	0.02
Be	0.15	Cr	0.06	Sc	0.11	Cu	0.01
Cr	0.12	Ti	0.04	Zr	0.09	Mo	0.01
Co	0.04	Al	0.04	Si	0.09	Co	0.00
Mn	0.02	Co	0.04	K	0.08	V	−0.03
V	0.01	Zr	0.03	Na	0.07	Si	−0.03
P	0.01	Be	0.03	Al	0.05	TOC	−0.03
Zn	−0.01	Pb	0.01	Zn	0.05	Ni	−0.04
Y	−0.03	TOC	0.01	Sr	0.01	Ti	−0.06
Cu	−0.03	Ba	0.01	P	0.00	Sr	−0.10
Ni	−0.04	Cu	0.00	Ti	−0.02	Be	−0.19
Sr	−0.06	V	0.00	La	−0.04	Al	−0.19
Mo	−0.07	Zn	0.00	Mg	−0.04	**Mg**	**−0.26**
TOC	−0.11	Ni	0.00	Ca	−0.09	**K**	**−0.26**
Pb	−0.13	Na	−0.01	Mn	−0.14	**Sc**	**−0.30**
Ca	**−0.28**	Mo	−0.02	**Ba**	**−0.24**	**Cr**	**−0.34**
Sum[1]	62.39		23.21		10.20		2.14
Sum[2]	62.39		85.60		95.80		97.93

Factor 1 = detrital.
Factor 2 = carbonate.
Factor 3 = TOC/redox.
Factor 4 = Na.
Sum[1] = %Sum of squares.
Sum[2] = Cumulative %Sum of squares.

Table 3
Q-mode factor analysis, WV core (sorted; without samples Si/Al >5).

Var.	Factor 1	Var.	Factor 2	Var.	Factor 3	Var.	Factor 4
Sr	**0.26**	**TOC**	**0.46**	**Ca**	**0.49**	**V**	**0.38**
Sc	**0.26**	**Mo**	**0.38**	**Mn**	**0.38**	**Mo**	**0.28**
Al	**0.26**	**Ni**	**0.36**	**Y**	**0.36**	Ni	0.19
K	**0.26**	**Na**	**0.30**	**Sr**	**0.33**	Ba	0.19
Ti	**0.26**	**Pb**	**0.24**	**Pb**	**0.20**	K	0.16
Mg	**0.25**	**V**	**0.23**	P	0.18	Ca	0.15
Be	**0.24**	**Ba**	**0.20**	TOC	0.18	Cr	0.14
Ba	**0.24**	**Si**	**0.20**	Fe	0.16	Sr	0.13
La	0.19	**K**	**0.20**	Sc	0.15	Mn	0.10
Si	0.17	Be	0.18	Mg	0.15	Cu	0.06
Zr	0.16	Ti	0.17	Ni	0.14	Zn	0.05
P	0.15	Zr	0.14	Cr	0.13	Sc	0.04
Y	0.12	La	0.14	Zn	0.13	Y	0.03
Fe	0.12	Al	0.12	Mo	0.09	Al	0.01
Na	0.10	Cr	0.11	Si	0.06	Be	0.00
Mn	0.10	Sc	0.09	Co	0.05	TOC	−0.01
Cr	0.09	Cu	0.08	Cu	0.04	P	−0.04
V	0.08	Co	0.07	Zr	0.04	La	−0.06
Co	0.03	Fe	0.07	Al	0.02	Ti	−0.10
Ca	−0.02	Mg	0.05	Be	−0.03	Mg	−0.10
Cu	−0.03	Zn	0.05	La	−0.05	Na	−0.12
Zn	−0.06	Y	0.02	K	−0.09	**Fe**	**−0.20**
Ni	−0.12	Sr	−0.03	Ti	−0.10	**Si**	**−0.25**
Pb	**−0.25**	P	−0.03	V	−0.10	**Zr**	**−0.32**
Mo	**−0.28**	Ca	−0.11	**Ba**	**−0.21**	**Co**	**−0.33**
TOC	**−0.38**	Mn	−0.13	**Na**	**−0.23**	**Pb**	**−0.50**
Sum[1]	48.01		42.66		6.30		1.42
Sum[2]	48.01		90.67		96.97		98.39

Factor 1 = fine-grained detrital; − TOC and redox.
Factor 2 = TOC/redox.
Factor 3 = carbonate; − Na and Ba.
Factor 4 = V and Mo; − Pb, Co, Si and Fe.
Sum[1] = %Sum of squares.
Sum[2] = Cumulative %Sum of squares.

Factor 2 is weakly associated with positive TOC/redox loading, with additional elements. The third factor represents the carbonate component in the system. A fourth vaguely defined, weak factor characterizes select redox-related elements (V and Mo) and a possible weak negative loading on coarse clastics and Pb.

Stratigraphically, proxy trends for the Akzo and West Valley cores indicate a complex set of interactions between detrital, TOC/redox, and carbonate components in mudrock-dominated facies. High TOC/redox concentrations low in the succession in Sequences 1 and 2 as well as Sequence 6, at least in part, marks relative starvation of clastic and carbonate sedimentation associated with sea level rise due to eustasy and orogenic loading. The successive rise of carbonate in Sequence 3, Skaneateles Formation, was in part a result of progradation of calcareous mud and silt downward along the cratonward ramp, along with minor in situ benthic shell production, and associated carbonate dilution of fine-grained clastics coming in suspension from the proximal basin margin. A decline in carbonate content upward through the Akzo and into the West Valley core marks the general increase of siliciclastic input from the proximal margin of the basin through time, and consequent dilution of carbonate. It also indicates migration of the cratonward basin margin out of the western New York region. The separation of clastic input into distinct alumino-silicate clay and quartz-rich sand factors (see Si/Al ratios in Figs. 5 and 6), which begins at the top of the Akzo core and continues upward through the West Valley core, indicates an overall trend toward progradation of sand-dominated facies, from the proximal margin of the basin, albeit with minor cyclic variation.

These complex relationships indicate shifts in sedimentologic inputs into the mudrock depositional system over time, through a range of scales. Domination of one or two factors, with resultant dilution of others, changes through time. The shifts are variously associated with relative water depth changes controlled by both eustatic and tectonic/sedimentologic processes, cratonward migration of the basinal trough and flanking cratonward and proximal ramps through time, progradation and retrogradation of the Catskill clastic wedge, and fluctuations in rates of orogenesis in the Acadian mountain belt.

4.2. Major proxies and their utilization in mudrock sequence stratigraphy

4.2.1. Total organic carbon (TOC)

The concentration of organic carbon in marine systems may be the result of multiple interacting factors, including sediment condensation, circulation changes, anoxia, increased nutrient availability and primary production, and burial efficiency (Arthur and Sageman, 2004). Much debate in recent years has focused on the roles of production versus preservation under anoxic conditions. However, sea level rise is clearly an important factor in TOC enrichment in shelfal/epicontinental sea settings (Arthur and Sageman, 2004).

The concentration of organic carbon through the Akzo and West Valley cores can largely be directly correlated with various scales of cyclicity within a sequence stratigraphic framework. TOC enrichment generally outlines the deepening successions through the transgressive systems tract, and generally into the lower part of the highstand systems tract. First order control of organic richness is associated with larger scale cyclicity. In the upper TST and lower HST of Sequences 1 and 2, concentrations of organic matter are consistently high (up to 17%); the overall trend of transgression and maximum depths (and varying degrees of condensation) swamps the system, and smaller scale fluctuations in relative sea level have little if any effect. During deposition of Sequence 5 in the upper part of the Hamilton Group, TOC drops to near zero levels throughout; again, lower levels of cyclicity have little effect on the concentration of organic materials, which appear to be consistently low owing to poor preservation potential under relatively oxic/aerobic conditions. In the intervening interval, however (e.g., Sequence 3, Skaneateles Fm., middle of the Hamilton Group cycle), numerous and varied fluctuations can be correlated with multiple levels of cyclicity superimposed upon the larger scale cycle.

4.2.2. Bioturbation/sediment fabric

Variations in sedimentary fabric (e.g., Cuomo and Rhoads, 1987; Droser and Bottjer, 1986), categorized as laminated, burrowed, and bioturbated textures, reflect the degree of infaunal (+/− epifaunal) biological activity. This variable serves primarily as a paleo-oxygenation proxy, generally interpreted to be associated with depth-related processes in epicontinental seas, and fits well within predictive sequence stratigraphic models (Savrda, 1991). Sediment fabric trends in this study show distinctive patterns throughout the mudrock succession. The proxy performs well under relatively low to moderate sediment input rates (e.g., on the western ramp and central trough of the basin); the pattern does, however, break down under conditions of rapid/episodic sedimentation in coarser, sand-dominated facies, associated with turbidite or tempestite deposition (e.g., Nunda Sandstone, West Valley core).

In this study, general trends in the degree of bioturbation, and ichnofacies, are interpreted to reflect depth-related changes in paleo-oxygenation. Shallower, well-oxygenated facies would be characterized by increased degrees of bioturbation, and more diverse ichnofossil assemblages (e.g., with *Chondrites*, *Planolites*, and *Zoophycos*). Intermediate depth facies, with lower levels of oxygen available would show a decrease in bioturbation, and be characterized by *Chondrites* with or without *Planolites* burrows). Deep water mudrocks, characterized by TOC-rich black shales, show no burrowing/bioturbation. Interpretations must, of course, be grounded by other lithologic and geochemical data; for instance, a decrease in bioturbation may also reflect increased sedimentation rates, not only decreased oxygen availability.

The Akzo core provides a detailed record of bioturbation and associated sedimentological and geochemical data. This allows for refinement of Hamilton sequence interpretation, which varies somewhat from that predicted by the Brett and Baird (1996) sequence model, which consistently placed the MFS close above basal sequence limestones. In this study, lower degrees of bioturbation are consistently found at a position a slightly higher in Hamilton Group cycles, interpreted here to indicate that the MFS occurs at a position higher in the sequences. Minimal bioturbation is generally associated with greater TOC enrichment, but in some cases (e.g., Sequence 3) they may not coordinate. We find that the record of bioturbation, in conjunction with other possible indicators (e.g., grain size, TOC concentration and possibly Ti/Al ratio), provides an effective and objective proxy for selecting the position of the MFS in dysoxic- to lower oxic-dominated sequences (Figs. 2–4).

4.2.3. Carbonate

The abundance of carbonate is controlled by several factors, including paleoenvironmental conditions and position in the sedimentary basin. Also important to this discussion are sedimentary dilution associated with high clastic input at times, and apparent exclusion of carbonate in TOC-rich facies (e.g., Sequence 2), possibly due to dissolution under acidic conditions associated with anoxia and redox processes (e.g., Reaves, 1986). Dissolution of carbonate is supported by the virtual absence of original pelagic carbonate (e.g., styliolinids and goniatite cephalopods are nearly always preserved as highly compacted molds) in condensed, TOC-rich strata. Hallock and Schlager (1986) report that in situ benthic carbonate sedimentation is minor at water depths greater than 100 m for Phanerozoic platform-type settings, which is within projected depths of 50–200 m for deeper parts of the Devonian Appalachian Basin (Vogel et al., 1987). We do note that clastic dilution may act upon carbonates (e.g., LHST), but also that the allodapic carbonate component may dilute fine-grained clastics in settings of low terrigenous input on the distal

cratonward ramp of a foreland basin (e.g., Sequence 3), or due to high benthic carbonate production in shallow, oxic facies (LHST of Sequence 3; Sequence 5).

Carbonate was a significant component of the sedimentary system throughout the Eifelian and Givetian stages in the lower to middle parts of the Akzo core. Regionally, carbonate concentration culminated with deposition of the Tully Limestone (represented in the Akzo core by the Taghanic unconformity), after which it sharply declined. Depth-related sedimentologic and paleoecologic conditions/processes, and basin geometry, form important controls on carbonate distribution through the succession. Maximum development of carbonate facies is associated with limestones at the base of sequences and subsequences. These have been interpreted to be skeletal concentrations associated with the shutoff of detrital input during the initiation of transgression in the early part of the TST, in settings shallow enough for carbonate production (Brett and Baird, 1996). Similarly, Cretaceous-age skeletal limestones that have indications of winnowing and condensation were interpreted by Sageman (1996) to be deposited during the LST to initial TST. Overall highest concentration of $CaCO_3$ in the Akzo core seems to occur in medial depth settings on the cratonward margin of basin (e.g., Sequence 3), where dilution by proximal-derived terrigenous sediments is minimized.

The dominant carbonate sediment type (benthic shelly, styliolinid, and micrite/calcisilt sediments) varies due to depth-related ecologic variations (Brett and Baird, 1996), and may assist in delineating sequence development. In strata of the Akzo core, macrobenthic skeletal carbonate is predominantly associated with more oxic, shallow water facies. Styliolinid-rich beds, associated with pelagic deposition of carbonate during the Devonian, are indicative of more basinal, deeper water facies. Micritic and calcisilt-rich beds mark intermediate settings.

4.2.4. Detrital-indicator geochemical proxies

The varying composition of detrital minerals supported by the results of Q-mode analysis, provides a useful proxy for determining clastic input into the mudrock depositional system. The element Al is most commonly utilized as a proxy for fine-grained sediments, because it is a major component of clay minerals. Additional elements related to clays in the fine-grained fraction include Na, Mg, Si (Si/Al<ca. 5), K, Be, and Sc; biogenic Si is a very minor component of these Devonian rocks. In contrast, the ratios of elements associated with coarser clastics, relative to Al concentration (e.g., Si/Al>ca. 5, Zr/Al and Ti/Al), provide proxies for silt- to sand-sized sediment input into the depositional system, although the concentration of some elements may also reflect other processes (e.g., volcanism, provenance/unroofing history; Dean and Arthur, 1998; Young and Nesbitt, 1998).

In this paper, we utilize Al as the primary indicator of fine-grained detritus, and a Si/Al ratio of >5 as a proxy for sand-dominated lithologies.

Deposition of coarser siliciclastic sediments in mudrock-dominated systems is largely due to riverine input into the basin. Some input, however, may also result from eolian, volcanogenic, biogenic, and diagenetic processes. Input from the first three of these latter sources may result from significant events, or be enhanced during a time of decreased terrigenous and/or carbonate sedimentation (e.g., condensed sections), as interpreted from bulges or spikes in Si/Al and Ti/Al ratios as seen in the upper part of the TST and EHST of Sequence 2, and corroborated by thin section petrology (Werne et al., 2002). Smaller scale variations in Ti/Al are used as a guiding proxy for relative degree sediment condensation, reflecting relative extent of enrichment of eolian silt during times of sediment starvation (Sageman et al., 2003).

Throughout much of the Akzo and West Valley cores, detrital sediments are characterized by mudrocks with a minor silt component occurring as background grains within mudstones and shales, or as uncommon, discrete siltstone to fine sandstone laminae or beds. Detrital elemental proxies (e.g., Al and Si) in those facies show a general positive correlation. Major separations of the detrital component into clay-silt sized (e.g., Al, Sc, K and others) and sand-sized (Si/Al>5 and Zr/Al) fractions first occurs near the top of Akzo core and again in middle to upper strata of the more distal West Valley core, due to progradation of the toe of the Catskill Delta complex across the northern Appalachian foreland basin. In addition, winnowing processes during LST or early TST may also lead to the concentration of sand/silt (e.g., high Si/Al ratio, near base of Sequence 5). Thus, short term shifts in Ti/Al ratios may reflect eolian input in condensed intervals; larger-scale shifts in Ti/Al such as that observed above 160 m in the Akzo core, reflect provenance-related changes in the adjacent Acadian Orogen.

4.2.5. Redox-indicator geochemical proxies

Elements that bond to organic matter or form sulfide compounds are enriched in strata under lower dysoxic to anoxic conditions. Concentrations of Mo, Mn, V, Cr, Ni, Co, Cu, U, and Th commonly parallel trends in TOC concentration (Calvert and Pedersen, 1996; Emerson and Huested, 1991; Jones and Manning, 1994; Sageman and Lyons, 2003; Tribovillard et al., 2006). Some, however, may also reflect other components and/or processes in mudrock dominated systems; for example, variations in elements such as Ni, V, and Cr, may also reflect unroofing history in the sedimentary source.

Tribovillard et al. (2006), in a review of paleoredox and paleoproductivity proxies, present U, V, and Mo, and to a lesser degree Cr and Co, as reliable indicators of redox conditions, due to their minimal association with detrital sediments. They also discuss the use of Ni, Cu, Zn and Cd as indicators of productivity, and note that Ba and P, commonly used as productivity proxies, can be unreliable owing to the fact that their concentrations may be altered by diagenesis.

Sageman and Lyons (2003) found a strongly positive covariance between the concentration and accumulation of TOC and Mo, due to appreciable enrichment of Mo under euxinic conditions relative to its concentration in oxic detrital sediments. Statistical analysis of the complete data sets from the Akzo and West Valley cores in this paper support that interpretation; in this paper we utilize Mo, along with TOC, as a proxy for redox/paleoxygenation conditions.

4.3. Interpretation of anoxic, dysoxic, and oxic sequences

To establish the utility of the various sedimentologic, paleobiologic, and geochemical proxies for sequence interpretation in mudrock facies, we must first analyze their trends through the three sequences of the Oatka Creek (anoxic-dominated), Skaneateles (dysoxic-dominated) and Moscow (oxic-dominated) formations of the Middle Devonian Hamilton Group.

4.3.1. Anoxic-dominated Sequence 2, Oatka Creek Formation: patterns and useful proxies

The base of Sequence 2 (Oatka Creek Formation; Fig. 2), is marked by thin limestones (Hurley and Cherry Valley members) that formed during initial transgression and shutoff of siliciclastic input into the basin. The latter carbonate (Cherry Valley Member) is characterized by abundant styliolinids and cephalopods, similar to condensed Devonian "cephalopodenkalk" limestones from Morocco and Europe (Bandel, 1974; Griffing and Ver Straeten, 1991; Tucker, 1974; Wendt and Aigner, 1985). Succeeding shale-dominated strata characterize much of the remaining sequence, with only minor limestones. Laminated fabrics are predominant through much of Sequence 2, as shown by Fig. 2; burrowed to bioturbated fabrics are predominantly associated with the basal transgressive limestones, and grade to laminated fabrics through overlying strata of the TST and HST.

High weight percentages of TOC in the Oatka Creek Formation, which range up to >17%, is representative of the relatively condensed late TST and EHST of Sequence 2 (Fig. 2). In the Akzo core the surface of maximum flooding is interpreted to occur at or near the position of

corresponding peaks in TOC and Mo and minima in siliciclastic proxies and $CaCO_3$, at approximately 336.9 m in the case of Sequence 2. Phosphorous data (not shown) also display peak values through the same interval. The interpretation is supported by a gamma ray peak of 800 api units at 336.5 m, which is an order of magnitude above background, and the disappearance of all burrowing at 336.8 m, resulting in a fully laminated sedimentary fabric.

Stable concentrations of Al, K, and related proxies above the MFS are interpreted to indicate EHST aggradation and stable input levels of fine-grained siliciclastic sediments. An anomalous positive bulge in the Si/Al curve through this interval may be related to non-riverine input of Si due to eolian, biogenic, or volcanogenic processes. Thin section analysis indicates the presence of numerous silt-sized quartz grains that may be of eolian origin, concentrated during periods of low sedimentation (Werne et al., 2002). Altered volcanic ash beds (K-bentonites), a source of silica, are reported from subjacent strata (Dennison and Textoris, 1970; Ver Straeten, 1996, 2004); only one locally occurring, apparent K-bentonite has been reported from Sequence 2 (Ver Straeten, 2004). Hosterman and Whitlow (1983) do note that some background sediments may be derived from ash deposition; background input levels of volcanogenic detritus are, however, undecipherable at present. Werne et al. (2002) interpreted the Si/Al and Ti/Al trends in this interval to indicate eolian input during a period of sediment starvation.

An overall increase in Al and associated proxies through the upper part of the sequence is indicative of fine-grained clastic progradation into distal portions of the basin during the LHST. A decrease in the Ti/Al ratio in the upper part of Sequence 2 (ca. 331 m) appears to signify increased clay input into distal, basinal environments during LHST, diluting condensed sediments associated with excess Ti and Si.

A carbonate peak high in the lower part of the Oatka Creek (Halihan Hill Bed of Ver Straeten, 1994, at 339 m), corresponds to the base of the TST of a prominent subsequence across the northern Appalachian Basin. Spikes in detrital input, with associated inverse changes in $CaCO_3$ and/or TOC content appear to correlate with the caps of smaller scale (fourth order and smaller) parasequence sets.

Overall, Depositional Sequence 2 and component systems tracts are characterized by a high degree of condensation and extreme anoxic, even euxinic conditions (Werne et al., 2002) associated, in large part, with a combination of rapid subsidence of the foredeep of the Appalachian Basin in the early stage of Acadian Tectophase II (Ettensohn, 1985; Ver Straeten, 1996) and a eustatic rise in sea level (T–R cycle Id of Johnson et al., 1985).

One significant anomaly in the sequence interpretation of strata from the Akzo core is the occurrence of the MFS above the Halihan Hill Bed. Other studies, based in eastern to central New York, place the Sequence 2 MFS in the East Berne Member, below the Halihan Hill Bed (e.g., Brett and Baird, 1996; Ver Straeten, 1996, 2007). Of significance locally, Ver Straeten et al. (1994) noted an anomalous development of shallower water facies in the Cherry Valley Member, relative to the underlying Hurley Member in outcrops approximately 30 km north–northeast of the Akzo core site — a reversal of basinwide sea level trends through the two members (Ver Straeten, 2007). This was interpreted by Ver Straeten et al. (1994) to reflect migration of a positive flexural feature through the area at the time of Cherry Valley deposition, related to foreland basin kinematics during early stages of Acadian Tectophase II. The flexural high likely continued to migrate through the vicinity of the Akzo core through deposition of the East Berne Member, prior to subsequent subsidence of the area with the passing of the bulge, resulting in local development of the anomalously late MFS.

4.3.2. Dysoxic-dominated Sequence 3, Skaneateles Formation: patterns and useful proxies

In general, proxy trends through Sequence 3 (Skaneateles Formation, Fig. 3) present a pattern of sequence development in a carbonate-rich, dysoxic-dominated mudrock succession. Following an initial rise and subsequent general decrease of TOC into the lower EHST (and anomalously in the upper TST), TOC remains relatively consistent through the upper EHST and LHST, moving back and forth across a line that defines one weight percent organic matter. This concentration represents a significant decrease relative to the average values for underlying Sequence 2, with a corresponding rise in weight percent $CaCO_3$.

As in Sequence 2, the base of Sequence 3 is, marked by a prominent limestone, characterized by high levels of bioturbation and $CaCO_3$, and a correlative decrease in all clastic proxies. Succeeding strata show an abrupt drop in $CaCO_3$, accompanied by increases in TOC, Mo, and clastic proxies. Maximum TOC, utilized in Sequence 2 and commonly recognized as an indicator of the MFS, occurs immediately above the basal limestone unit. This interpretation is, in a broad sense, supported by trends in bioturbation; those trends, however, are more ambiguous, with laminated intervals occurring close above the basal bounding limestone and again through a TOC-poor interval near 310 m. The entire interval between the basal limestone (at ca. 330 m) to the base of the 310 TOC-poor interval marks the TST. The TOC maximum immediately above the basal limestone unit likely represents a fourth-order or smaller scale (subsequence) MFS.

Five distinctive phases of deposition characterize Sequence 3 above the basal sequence-bounding limestone. Three to four positive to negative excursions in clastic proxies, up to 309 m, indicate cyclic clastic versus carbonate deposition. Upward into the stable, carbonate-dominated second phase (309–299 m), detrital input is swamped by fine-grained carbonate (micrite–calcisilt carbonate type). This interval of consistently low detrital sedimentation may represent an aggradational EHST phase or, alternately, fourth-order LHST dilution of clastic proxies within a lower subsequence by carbonates prograding from the western, cratonward margin of the basin. Brett and Baird (1996) and Baird et al. (2000) support the latter interpretation, attributing decreasing terrigenous content to dilution by carbonate delivered to the basin from a cratonward source during a smaller scale, perhaps fourth or fifth order, shallowing event.

A return to cyclic alternations of clastic indicators and $CaCO_3$ in phase 3 (above 299 m) is associated with a general rise in detrital input. This rising trend peaks near the upper part of the sequence with a relatively smooth positive rise in clastic proxies (267–258 m), which indicates maximum clastic dilution and swamping of carbonate during the late stage of the LHST/falling stage. The uppermost phase of Sequence 3 (258–251 m) is marked by abrupt declines in bioturbation and clastic indicators and a rise in the concentration of TOC and redox-related proxies. This interval represented by the Butternut Black Shale Member in central New York State undoubtedly records a fourth-order late TST to HST but its appearance so high in the third-order sequence seems anomalous.

The abundant small-scale alternations of terrigenous material and carbonate, indicated by zigzag curves in both TOC and $CaCO_3$, reflects cyclic dilution of carbonates by terrigenous clastics and vice versa associated with smaller scale cyclicity. Low in the section (deposition phases 1 to 2), cratonward-sourced carbonate fines diluted siliciclastic muds which were not yet efficiently transported from the proximal clastic sourceland across a central basin trough; higher in the section, within the third-order sequence LHST, the carbonate became diluted by clastic muds as fine-grained facies were finally able to expand cratonward beyond the central basin trough.

Carbonate type displays a distinctive upward shift through Sequence 3. A mixed pelagic–benthic macro-skeletal rich limestone marks the base of the sequence. Succeeding fine-grained micrites and/or calcisilts decrease above deposition phase 2, initially replaced by styliolinid-rich limestones, followed by a return to calcisilt–micritic beds. Macroskeletal carbonate comprises an increased, but still minor component, of the uppermost part of Sequence 3, and

then dominates the coral- and crinoidal-rich, basal TST limestone of Sequence 4.

Bioturbation data from Sequence 3 indicate more extensive burrowing of sediments than in Sequence 2, with a distinct maximum at and adjacent to the lower and upper sequence boundaries. Individual peaks in the bioturbation index within the HST are associated with carbonate-rich beds, which may also feature benthic forms indicative of relatively deep water, dysaerobic Hamilton biofacies (e.g., *Ambocoelia*-chonetid biofacies of Brett et al., 1990, characterized by small brachiopods and auloporid corals).

Overall, sedimentologic and biologic proxies show concordance with secular trends in third order sea level changes in that peak values in $CaCO_3$ and bioturbation occur immediately above the sequence boundary. As noted, however, proxies also track subsequence (fourth-order) scale divisions and smaller scale patterns of cyclicity, creating a complex series of signals throughout Sequence 3, especially in the record of bioturbation, TOC, and the interaction of carbonate and detrital sediment.

General models of LHST deposition predict increased terrigenous input, a higher degree of bioturbation, and dilution of carbonate by siliciclastics, along with dilution and/or destruction of TOC during a fall in relative sea level. As predicted, $CaCO_3$ decreases through most of the upper part of the Skaneateles Formation. Interestingly, however, the degree of bioturbation also decreases throughout much of the LHST, and % TOC remains at approximately 1% through the upper part of the LHST. In the interval immediately subadjacent to the sequence boundary, an increase in TOC occurs in conjunction with increased $CaCO_3$; these two parameters are generally in opposition to each other, a relationship that is maintained throughout the sequence, but breaks down in the upper LHST. In general, trends through the uppermost LHST (phase 5) of Sequence 3 do not fit into most predictive sequence models. Rising carbonate and TOC concentrations, accompanied by decreasing detrital signals present an enigmatic lead-in to the basal limestone at the base of Sequence 4. Though not visible in the core, a sharp shift in most proxies at the top of the LHST TOC-rich interval (at ca. 252 m) correlates with the position of a locally to regionally significant sequence-bounding unconformity (Baird et al., 2000), eroded top-down to a position close to the TST of the upper subsequence. This accounts for the anomalous LHST TOC-rich interval.

4.3.3. Oxic-dominated Sequence 5, Moscow Formation: patterns and useful proxies

Selected proxies that helped to define systems tracts in Sequences 2 and 3 are less useful in the more oxic and more clastic-rich Sequence 5 (Moscow Formation; Fig. 4). Increasing sedimentary dilution of carbonates by fine-grained clastics through the TST to middle HST of the Moscow Formation is indicated by a trend toward decreased carbonate and increases in detrital proxies. This interpretation is supported by opposing Al versus Ca trends though the interval. However, these patterns do not help to clearly delineate systems tracts within Sequence 5. In addition, the general lack of change in TOC content and associated redox indicators (e.g., Mo), a result of the generally oxic depositional environments and a high degree of biogenic activity, renders such proxies useless in delineating sequence development in oxic Sequence 5. Similarly, due to a generally higher input of siliciclastic sediments in the late stage of the larger scale Tectophase II cycle, there are fewer shifts in the concentration of clastic proxies upward through the sequence to help distinguish Sequence 5 systems tracts.

Sedimentary fabrics, however, show a distinctive pattern of change through the Moscow Formation. The degree of bioturbation declines up to a position about a third of the thickness up the formation, to a position that may be defined as the MFS, and the TST–EHST boundary, and then fluctuates back and forth at the scale of apparent fourth and smaller order cycles. This appears to indicate that in relatively shallow, oxic mudrock settings similar to the Moscow Formation, bioturbation trends may be the best indicator of the development of the sequence and its component systems tracts.

Uppermost strata of Sequence 5 again show an anomalous minor enrichment of TOC and decreasing detrital content, similar to the highest LHST deposits of Sequence 3. In outcrop this event is represented by a dark gray, unfossiliferous mudstone to shale, the Gage Gully beds of Brett and Baird (1994), which has been interpreted to represent an anomalous deepening event in the upper LHST (Brett and Baird, 1996, 2003) prior to the major lowstand of the Tully Limestone. An alternate interpretation by Brett et al. (this issue) proposes that this interval of TOC enrichment may represent the late TST or early HST of an additional third-order sequence that includes the upper Moscow and lower Tully formation strata.

4.4. Middle to Upper Devonian mudrock sequence stratigraphy — additional sequences

The remaining mudrock-dominated sequences in the Akzo and the succeeding West Valley cores (Sequences 4 and 6–11, Givetian to lower Famennian stages) can be examined utilizing the multi-proxy approach established for Sequences 2, 3, and 5 (data in Figs. 5–7; sea level curve and sequence framework in Fig. 7). These data account for changes in depositional trends and sediment input, and the resulting shifting signals in the various sedimentologic, paleobiologic, and geochemical proxies.

4.4.1. Sequence 4: Ludlowville Formation, Hamilton Group

The base of Sequence 4 is marked by the Centerfield Limestone, a regionally widespread carbonate bed (Figs. 5 and 7) that overlies the anomalous LHST organic-rich interval at the top of Sequence 3. The top of the sequence is placed at the base of the next overlying major limestone at the base of the Moscow Formation.

A quick survey of proxy trends through Sequence 4 (Fig. 5, Ludlowville Fm.) indicates generally low TOC and Mo, with an overall higher degree of bioturbation relative to underlying Sequences 2 and 3. Carbonate content is also decreased relative to the lower sequences, accompanied by increased Al and Si and overall decreased Si/Al values. For most of the sequence TOC remains below 1%, but rises toward the middle of the sequence, followed by an overall decline upward, creating a relatively symmetrical TOC trend through the formation. Bioturbation, as would be predicted, shows a directly opposing, relatively symmetrical trend. Mo and other redox-related proxies (not shown) remain relatively low, rising only toward the middle, relatively TOC-enriched interval of the formation. The latter appears to reflect developments within a fourth-order cycle.

Following initial high concentrations, $CaCO_3$ declines to relatively low levels, with only a very subtle rise visible through much of the Ludlowville sequence. Detrital proxies display a rise through the interval immediately above the basal sequence-bounding limestones, followed by overall decline. The decline is most pronounced in uppermost strata, where $CaCO_3$ undergoes a more distinct rise, associated with increased skeletal carbonate visible in the core.

4.4.2. Sequences 6–10 Overview

Proxy trends in TOC, Mo, bioturbation, $CaCO_3$ and detrital proxies (Al and Si/Al) outline the development of sequences through upper Givetian to lower Famennian strata (Geneseo to Gowanda formations; upper part of Figs. 5 and 6). One notable trend is the decline of $CaCO_3$ through Sequences 6 to 7, to relatively low concentrations (generally $<5\%$) through the rest of the succession.

TOC/Mo and bioturbation, as previously, maintain a generally negative relationship. With the decline of significant $CaCO_3$ input (of all carbonate types), Al and Si/Al curves show a subtle decoupling that increases upward, most notably in uppermost samples of the Akzo

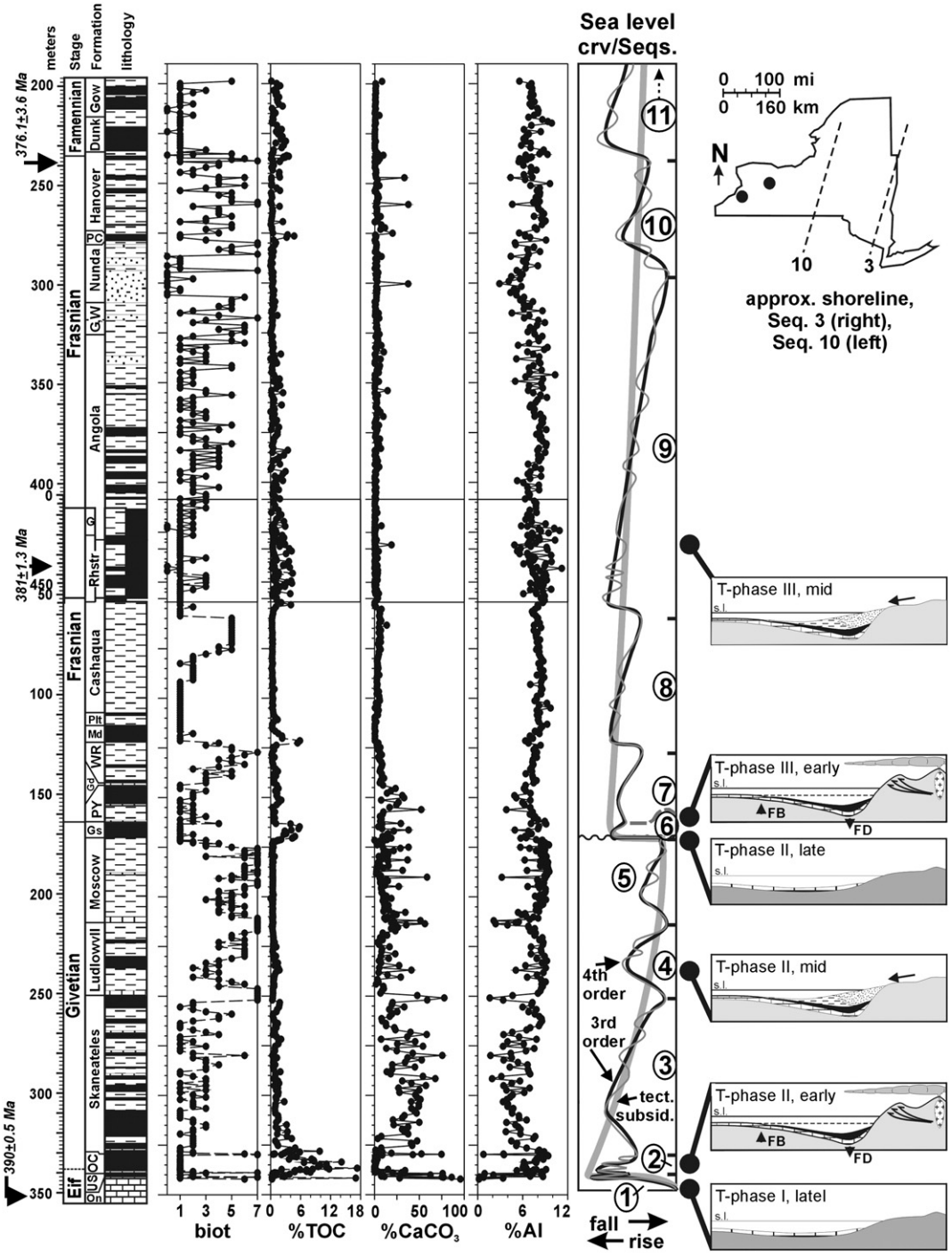

Fig. 7. Overview of mudstone-dominated Akzo and West Valley cores, with stratigraphy, key proxy trends, interpreted relative sea level and subsidence curves, and Acadian tectophase development. Map in upper right shows approximate position of shoreline during Sequences 3 and 10 (based on chart from Rickard, 1975). Overlap of cores in Rhinestreet Fm. correlated at base of Corning black shale tongue (based on TOC trends). Abbreviations: as in Fig. 1, plus T-phase = Tectophase (of Ettensohn, 1985); s.l. = sea level; tect. subsid. = tectonic-induced subsidence.

core and in the Nunda Formation, near the base of the upper third of the West Valley core.

The proxy trends outline a series of alternating higher TOC and Mo versus higher, and at times coarser, detrital and bioturbation values. The trends outline six significant post-Hamilton sequences through the Akzo and West Valley cores (Fig. 7). The sequences in general show a greater similarity to the dominantly anoxic to dysoxic Sequences 2 and 3, differing most notably in the lower carbonate content. In addition, vertically shifting relationships between proxies indicate evolving depositional conditions and basinal configuration through the upper Givetian to lower Famennian of the northern Appalachian Basin.

4.4.3. Sequence 6: Geneseo and lower part of Penn Yan formations, Genesee Group (upper Givetian)

Sequence 6 is a relatively thin, condensed sequence, dominantly comprised of black shales with interspersed thin limestones. Regional study indicates that most of the TST, largely represented by the Tully

Limestone, is absent at the Taghanic Unconformity. A prominent, widespread pyritic–phosphatic lag deposit (Leicester Pyrite; 171.55 m of Akzo core), reworked from upper strata of the underlying sequence, marks the position of the unconformity.

Proxy trends through Sequence 6 show a character and development similar to the dysoxic-dominated Sequence 3. TOC, $CaCO_3$, and bioturbation appear to be most useful in delineating the development of the sequence, although the generally negative relationship between TOC and bioturbation becomes erratic in the upper part. As previously, the Si/Al ratio is notably elevated in TOC-rich and Al-/$CaCO_3$-poor intervals in the lower part of the sequence.

Delineating the systems tracts within Sequence 6 is relatively complex. Tentatively, the TST and EHST boundary is placed just above the lower interval of TOC-rich strata (at ca. 169 m), below the mid-Geneseo (Fir Tree Member) limestones. Under this interpretation the LHST lies between those limestones and the top of Sequence 6. However, the lower part of the sequence may be missing in this region, due to condensation and sediment starvation; a lower position for the third-order MFS is likely. A set of thin limestones (Lodi Member) mark the base (LST) of the succeeding Sequence 7.

Two prominent subsequences are visible within the data set, divided by an interval of thin, styliolinid limestones (Fir Tree Member). The uppermost of the limestone beds (at 166.6 m) contains a mix of pelagic styliolinid and benthic macroskeletal carbonate types. In the same interval in the mid-continent U.S., Day et al. (1996) recognize the same two cycles, but interpret them to represent separate sequences (T–R cycles IIa-1 and IIa-2).

4.4.4. Sequence 7: upper Penn Yan Formation, Genundewa Member, and West River Formation (uppermost Givetian, lower Frasnian)

Sequence 7 is developed through a succession of shales and mudstones, minor limestones, and silty shales to mudstones of the upper part of the Penn Yan Formation, the Genundewa Limestone, and West River Formation. Proxies throughout the succession indicate dominantly dysoxic conditions similar to Sequence 3. With fluctuating relationships between carbonate and detrital proxies through the succession, bioturbation perhaps provides the best outline of sequence development.

The base of Sequence 7 is marked by slightly fossiliferous, bioturbated limestones (Lodi Member), with a mix of pelagic styliolinids and benthic macroskeletal material of crinoid ossicles, auloporid corals, and ambocoeliid brachiopods. This represents the base of the TST, developed with a transgressive shutdown of clastic influx into the basin. A phosphatic lag bed capping the top Lodi Limestone at 163 m, a succeeding decline in bioturbation, and a slow rise in TOC concentration (to 154 m) is associated with subsequent development of the TST. A subtle erosion surface is visible in the core at 158.1, close below a return to fully laminated facies. This may mark a maximum starvation surface within the TST.

The succession above maximum TOC initially features cyclic alternations of carbonate and fine-grained detrital proxies, showing an overall decline in $CaCO_3$ and a rise in detrital indicators. This appears to represent an EHST. A succeeding gradual, steady decline in carbonate to very low levels and rising concentrations of Al and associated fine-grained detrital indicators (beginning at 144 m and increasing to ca. 125 m) mark LHST to perhaps basal LST conditions. This interpretation is supported by bioturbation trends undergoing a significant, steady rise through the upper part of the sequence to 127 m.

Sequence 7 is divisible into two major subsequences. The base of the upper subsequence occurs closely below or at the Genundewa Limestone, a thin, pelagic-type carbonate unit directly analogous to limestones at the bases of Sequences 2 through 4.

One of the more significant overall trends within Sequence 7 is the upward decline of $CaCO_3$ above the Genundewa Limestone. This results in a greater separation and decreased correlation between detrital proxies, including that between Al and Si (shown by Si/Al ratios). In overlying sequences this is marked by significant disparities between the latter two proxies, indicative of increased silt- to sand-sized input into the area, most notably in Sequence 9. The decline in carbonate concentration through Sequence 7 appears to be associated with migration of the basin axis into the area of the present-day Genesee River Valley at that time, and increased progradation of proximally derived muddy sediments. Carbonate content and type, useful as indicators of sequence development lower in the succession, decline in their utility.

4.4.5. Sequence 8: upper West River, Middlesex, Pultney, and Cashaqua formations (lower Frasnian)

Sequence 8 comprises the upper part of the West River Formation (Genesee Group) and the Middlesex, Pultney, and the bulk of the Cashaqua formations (Sonyea Group). The strata consist primarily of medium to dark gray shales (TOC<1%), with a widespread black shale (Middlesex Formation) low in the succession, and a generally low degree of bioturbation. In this sense, Sequence 8 is again broadly similar to Sequence 3, representative of dominantly dysoxic environments.

The basal sequence boundary is gradational, with no indication of unconformity. The LST appears to be bounded bottom and top by the beginning of relatively stable, high background levels of detrital indicators and bioturbation at or shortly above 132 m, and a decline in bioturbation and succeeding rise in TOC concentration beginning at about 126 m. A pyritic bed, with an apparent erosion surface at its base (Williamsburg Bed), and shift from mixed green and medium dark gray shale to grayish black shale may represent a 'maximum starvation surface', formed during the time of the maximum rate of base level rise.

The top of Sequence 8, may occur close to the base or top of an interval of stable values of bioturbation (rank value = 5), succeeded by an immediate shift to fully laminated facies. The former should mark the position of the LST; the latter position, at the abrupt shift from bioturbated to laminated textures, appears to indicate a position within the TST.

In contrast to the complexities of distinguishing systems tracts within Sequence 6, the proxies outline a relatively simple and easily interpretable depositional framework. LST deposits appear to be represented by high background levels of detrital indicators and bioturbation between 132 and 126 m in the Akzo core. Succeeding cyclic declines in bioturbation, $CaCO_3$ and Al, accompanied by a rise in TOC–Mo and Si/Al above 126 m appear to mark a turnaround at the base of the TST. Peak TOC and Mo, paralleled by a drop to lowest values for detrital input and bioturbation in the lower to middle Middlesex Shale, point toward the position of a maximum flooding zone at the top of the TST.

A return of detrital and carbonate indicators to levels comparable with sub-Middlesex strata, although not accompanied by an analogous rise in bioturbation, is interpreted to mark the lower EHST. Generally stable, if punctuated detrital Al values through the remainder of the sequence are not of assistance in distinguishing aggradational from progradational processes. Carbonate, and/or bioturbation, may be of greater assistance; following a subtle, spiked background level of approximately 3%, $CaCO_3$ concentrations show a subtle rise above 90 m, accompanied by an initially slow, stepped rise in bioturbation up to stable, peak values beginning at 73 m. These intervals appear to mark the two divisions of the HST. Succeeding strata are placed within the LST of overlying Sequence 9.

Sequence 8 appears to be divisible into three subsequence-level units, with their bases positioned at 132 m, 106 m, and 82 m.

4.4.6. Sequence 9: upper Cashaqua, Rhinestreet, Angola, Gardeau, West Hill and lower to middle Nunda formations (middle to upper Frasnian)

Sequence 9 is developed through a thick (ca. 160 m-thick) succession of silty mudstones, black shales (Rhinestreet Fm.), and

interbedded dark gray and green mudstones that coarsen upward into very fine to fine sandstones (Nunda Fm.). Carbonate content generally remains at insignificant levels; distinctive patterns in TOC and decoupled fine- and coarse-grained clastic components sharply outline sequence development, also distinguished by trends in bioturbation. The succession ranges from anoxic/dysoxic fine-grained basinal facies to fully oxic, sand-dominated shallow ramp deposition.

Upper strata of the Akzo core comprise the LST, TST and lower EHST of Sequence 9. Overlap of the Rhinestreet Formation allows correlation between the Akzo and West Valley cores, using the widespread fourth and uppermost Corning black shale tongue of the Rhinestreet Formation. The upper part of the TST and overlying systems tracts of Sequence 9 are interpreted from data of the West Valley core.

A long, stable degree of bioturbation of 5 in the upper Cashaqua Shale and a lack of obvious trends in detrital and carbonate concentrations make it difficult to pick a base for the sequence boundary. Large burrows and thin limestone beds in the interval around 61–62 m (Akzo core) may imply shallowest water conditions within the succession, and initial detrital starvation at the turnaround to sea level rise; the base of the TST may occur at approximately 62 m (Akzo core), at the lowest of a four thin, highly bioturbated limestone beds beginning 3 m below the start of laminated facies. An ensuing decline in detrital proxies and carbonate into the lower part of the Rhinestreet black shale marks the remainder of the TST. A transition from TST to EHST is not easily discernible in the data, but may lie close to maximum TOC (550 m, West Valley core). Fine-grained proxies (Al and others) show a subtle slow rise through the overlying lower Angola shales, associated with declining TOC concentration through the EHST.

At approximately 380 m (West Valley core), Al begins an overall decline as Si and Si/Al ratio begin a long, gradual rise upward to a peak in Nunda Sandstone. This appears to reflect progradation of sand-rich facies into western New York during LHST.

Patterns of bioturbation show a predictable decrease above the LST to lows in the TST and lower EHST, with a gradual, punctuated rise into and through the LHST. However, within the upper LHST and the succeeding LST of the Nunda Sandstone, bioturbation abruptly shifts from 7 (highly bioturbated) to 1–2 (laminated), or is not visible (=0). Burrows through this interval generally consist of long, vertical forms, interpreted to be fugichnial (escape) burrows. These data reflect very high sedimentation rates during a major progradation of sand facies, which at times outstripped the ability of burrowing organisms to keep up with accumulation of sediments.

4.4.7. Sequence 10: middle to upper Nunda, Pipe Creek and most of Hanover formations (upper Frasnian)

A sharp rise in Si/Al values beginning within a meter of the base of the Nunda Formation initiates a transition into increasing silt- to sand-rich facies, with a maximum ratio approaching eight at approximately 300 m. The sandstones appear thick bedded to massive with laminated or homogeneous internal fabric and upper fine sand size, the maximum recorded grain size. This interval is interpreted to have been deposited across the deeper central trough of the basin in western New York during lowstand conditions of Sequence 10.

Different positions can be chosen for the base of the TST on the basis of different characteristics. The maximum value of Si/Al (8.52), reflecting greater quartz sand content, occurs at approximately 300 m. This high falls within an interval of thick-bedded to massive sandstones with no internal fabric. A second potential base to the TST (ca. 288 m) occurs at the top of an interval of cross-bedded sandstones and siltstones, appearing to represent significant hydrodynamic energy. Alternatively, a sharp shift at 286 m from laminated and indistinguishable fabrics to highly bioturbated textures could be interpreted to represent the base of transgression. A succeeding shift to siltstones, with thin, macroskeletal limestones (analogous to Hamilton basal TST limestones), small limestone concretions, and fine glauconite at 285 m indicate a position within the TST. Peak concentration of TOC, in this case decoupled from maximum values for Mo, occurs within black shales of the Pipe Creek Formation (at ca. 276 m).

Above peak TOC concentration, Al is seen to rise and remain relatively stable through the lower part of the Hanover Formation, excepting sharp negative spikes associated with carbonate-rich beds. Decreasing Al above 251 m is accompanied by rising Si and Si/Al values. These two trends of Al concentration appear to mark the EHST and LHST of Sequence 10.

4.4.8. Sequence 11: uppermost Hanover, Dunkirk, and Gowanda formations (uppermost Frasnian, lower Famennian)

Upper strata of Depositional Sequence 11 were not analyzed in the West Valley core, and so the full sequence cannot be interpreted. The LST, if present, is represented by a thin interval (ca. 2–3 m-thick) of siltstones to very fine sandstones near the top of the Hanover Formation. Maximum recorded grain size (very fine sand) at 238.75 may record maximum lowstand conditions. The apparent base of the TST (ca. 238.3 m) is associated with a shift to siltstones and black, TOC-rich strata (increased TOC, Mo) and decreases in Si/Al and the degree of bioturbation. A lack of data above 187 m precludes delineation of the boundary between the TST and EHST and subsequent parts of the sequence.

The Frasnian–Famennian stage boundary lies 1.3 m above the base of the TST of Sequence 11, in uppermost strata of the Hanover Formation (Over, pers. comm.). This is the position of the Late Devonian Upper Kellwasser mass extinction horizon.

4.5. Relationship of sequences to Devonian T–R cycles

The preceding interpretation presents a refinement of previous Devonian cyclic interpretations for Eifelian to Famennian strata of the Appalachian Basin (e.g., Brett and Baird, 1996; Brett et al., this issue; Dennison and Head, 1975; House and Kirchgasser, 1993; Johnson et al., 1985, 1995; Ver Straeten, 2007; Fig. 8). One of the key changes in this paper is placement of many sequence boundaries at a lower position than for Johnson et al.'s (1985) T–R cycles. The latter authors in many cases placed their T–R cycle boundaries at major flooding surfaces (typically maximum starvation surfaces), which occur well up in the TST of a sequence.

Two examples of these refinements are seen in Sequences 1 and 2, which correspond to T–R cycles Id and Ie of Johnson et al. (1985). Ver Straeten (1996, 2007) has shown that the base (LST) of Cycle 1 lies in the upper part of the Moorehouse Member of the Onondaga Formation. The overlying Seneca Member and lower part of the Bakoven Member of the Union Springs Formation represents the TST of Cycle 1. This contrasts with Johnson et al.'s placement of the base of T–R cycle Id at the base of the Union Springs Formation. The base of Cycle 2 (Oatka Creek Fm.) is placed at the base of the Hurley Member (Chestnut Street Beds) of the New York succession, a short distance below the position chosen by Johnson et al. (1985).

Sequences 3, 4, and 5 discussed herein were lumped together by Johnson et al. (1985) as T–R cycle If. This was in part due to the generally shallow, regressive nature of the upper part of this succession in many cratonic basins, represented by shallow peritidal facies and/or widespread subaerial exposure and erosion. Not recognized by Johnson et al. (1985) was the well developed character and preservation of those cycles/sequences in the Appalachian Basin (Ludlowville and Moscow formations). Brett et al. (this issue) propose that the term Cycle If be restricted to the Skaneateles Formation, and that three additional T–R cycles be added to the Johnson et al. (1985) framework, T–R cycles Ig, Ih and Ii, represented by Ludlowville, lower to middle Moscow, and upper Moscow to lower Tully formations. Their proposed latter sequence/T–R cycle Ii is not recognized in this paper. This is in part due to the absence of the Tully Limestone

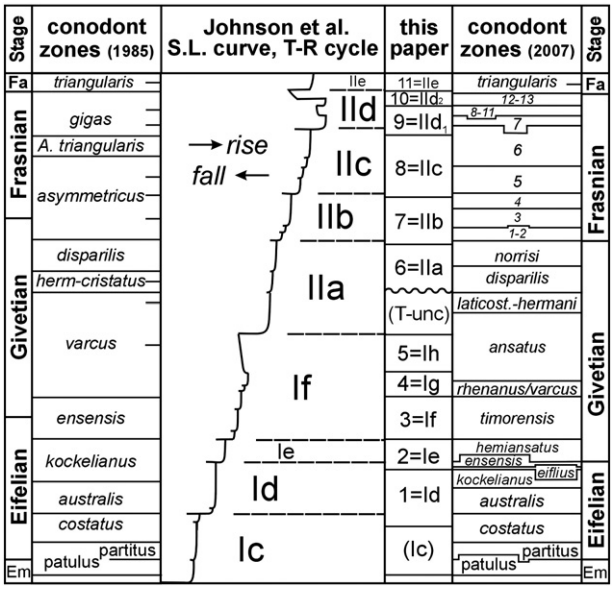

Fig. 8. Comparison of depositional sequences 1–11 with Devonian T–R cycles of Johnson et al. (1985). Note basal positions of Sequences 1, 2 and 7–11, which represent refinements of their respective T–R cycles. New T–R cycles (Ig and Ih) equivalent to Sequences 4 and 5 from Brett et al. (this issue). Division of T–R cycle IId in agreement with Day (1998). Conodont zones after Johnson et al. (1985), Kirchgasser et al. (1994), and Kaufmann (2006). Abbreviations: Ems = Emsian; Fa = Famennian; *laticost.* = *laticostatus*.

in the Akzo core at the Taghanic unconformity. The upper Moscow (Spezzano and Gage Gully beds interval) is treated herein as a subsequence (fourth-order sequence) within Sequence 5/T–R cycle Ih.

Similarly, we differ from Johnson et al. (1985) in the recognition of two separate sequences within their T–R cycle IId. This subdivision follows along Day (1998), who recognized two third order sequences within this cycle. Unlike Day et al. (1996), however, we have not split our Sequence 6 (= T–R cycle IIa of Johnson et al., 1985) into two separate sequences.

5. Summary and conclusions

5.1. Multi-proxy analysis of sequences and systems tracts in mudrock-dominated facies

The application of a multi-proxy analytical methodology, incorporating sedimentologic, paleobiologic, and geochemical data sets, helps delineate the developmental history of stratigraphic sequences in fine-grained clastic facies. In this study, the application of such data sets to Devonian strata helps refine the sequence stratigraphic framework for established sequences in the Middle Devonian of New York State, and to delineate additional, less clearly defined ones in the Upper Devonian. A total of 11 major ("3rd order") sequences and numerous smaller-scale cycles are recognized between the middle Eifelian to lower Famennian (ca. 15 m.y.) in the northern Appalachian Basin. These sequences are superimposed on two larger scale tectophase cycles that are related to orogenic activity on the eastern margin of North America at that time.

A series of sedimentologic, paleobiologic, and geochemical proxies (e.g., lithology, grain size and carbonate type; faunal/ichnofaunal data and degree of bioturbation; and concentrations of trace elements, TOC and $CaCO_3$) proved to be useful in reconstructing sequences and their component systems tracts. The usefulness of proxies varies among sequences dependent on depositional, paleoceanographic, paleoecologic, and early diagenetic conditions. Those proxies that show a range of variations in specific settings, such as grain size, degree of bioturbation, and concentrations of TOC and elements/elemental ratios (e.g., $CaCO_3$, Al, Ti, Mg, Sc, Si, Mo, Ni, V, Si/Al and Ti/Al) may help delineate depositional dynamics related to redox conditions, condensation, dilution, and clastic, biologic, and/or authigenic sediment sources (Figs. 9 and 10).

In fine-grained, anoxic-dominated conditions that are interpreted to represent relatively deep, basinal settings, sequences and systems tracts are best delineated by redox-related proxies TOC and Mo. Bioturbation, which shows a strong negative relationship to TOC and Mo, may only be of assistance at the lower and upper margins of anoxic sequences, during the LST, basal TST and LHST. The concentration of Al, as a proxy for fine-grained clastic input, helps distinguish EHST and LHST. Si/Al within oxygen-restricted, basinal sequences generally shows enrichment in more TOC/Mo-concentrated intervals, apparently reflecting a relative increase of eolian, volcanic or diagenetic inputs associated with condensation or a lack of dilution of these components.

Under intermediate, dysoxic-dominated conditions TOC/Mo, bioturbation, and Al remain effective indicators of sequence development. In relatively oxygenated, mudrock-rich and carbonate poor sequences, with no significant deposition of coarser clastic sediments, bioturbation may function as the most effective proxy for recognizing systems tracts.

In mixed fine-grained, clastic-carbonate successions, the concentration and type of $CaCO_3$ (e.g., benthic macroskeletal, pelagic styliolinid/dacryoconarid, and micritic/calcisilt) is affected by changes in water depth during the development of sequences, and is useful in identifying position within multiple scales of cycles. High concentrations of $CaCO_3$ are generally focused in sequence/subsequence bounding limestones associated with initial transgressive deposits. However, carbonate concentration and type is affected by numerous processes that may be depth-related, including, dilution by high terrigenous input rates, exclusion by ecological factors, or possible dissolution in anoxic facies. Carbonate may also dilute the concentration of fine-grained clastics in late HST by high micrite/calcisilt input in distal, dysoxic facies or fine- to medium grained clastics (mud to sand) and by abundant benthic shelly material in more oxic facies. Deeper, more basinal conditions, often associated with anoxia to dysoxia, show a dominance of pelagic carbonate. In contrast, decreased depth and greater oxygen availability lead to an increase in macroskeletal carbonate. In intermediate depth/oxygenation settings, micrite to calcisilt tend to dominate $CaCO_3$ deposition. Carbonate type is also strongly affected by paleogeographic position within the sedimentary basin, especially in foreland basins.

In more proximal, carbonate-poor successions, fine- and coarse-grained fractions become increasingly differentiated, as indicated by relatively high Si/Al ratios (Si/Al ≥ ca. 5). In contrast to more basinal sequences, the high Si/Al values reflect deposition of coarser clastics during LHST and LST, with or without reworking in the basal TST. Relatively increased TOC values may still be useful in delineating the TST. Bioturbation is, as noted, an effective proxy for oxygenated portions of sequence and systems tracts development in proximal, more fully oxic settings. It must be noted, however that bioturbation may become swamped due to high sediment input rates during the LHST or LST, leading to laminated or massive, undifferentiated fabrics (bioturbation = 1 or 0, respectively).

Elemental ratios indicative of coarser clastic input (e.g., Si/Al, Zr/Al and Ti/Al) also are applicable to identifying position within a sequence (LHST and LST); however, in distal, condensed settings, notably within the TST, enrichment of the coarser fraction may also occur associated with normal background eolian, volcanogenic, or biogenic processes.

As predicted, fluxes of siliciclastic, carbonate, and organic sediment types vary with depth, and therefore between sequences and systems tracts. Any of them can be shown to dilute the concentration of the others through different stages of sequence development. Therefore, concerns of relative availability of the different sediment types must

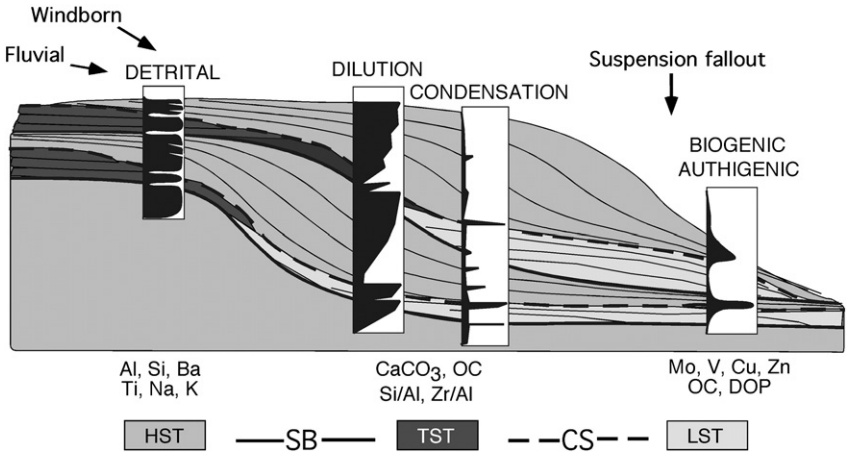

Fig. 9. Geochemical proxies for recognizing systems tracts. Sedimentologic, paleobiologic, and geochemical proxies useful in reconstructing sequences and their component systems tracts in mudrock dominates facies. Usefulness of proxies among sequences dependent on depositional, paleoceanographic, paleoecologic, and early diagenetic conditions, related to redox conditions, condensation, dilution, and clastic, biologic, and/or authigenic sediment sources. Dark areas of boxes show relative importance of detrital input, dilution, condensation, and biogenic/authigenic input through the development of sequences.

be examined carefully in interpreting relative depth and position within a sequence.

5.2. Eifelian to lower Famennian sedimentation and basin development

The broadest outline of sedimentation patterns recognized herein can be briefly summarized as follows.

1. Basinwide deepening due to tectonic-induced subsidence (Acadian Tectophase II) and eustatic sea level rise (Ver Straeten, 2007). Deposition of condensed, TOC-rich sediments occurred through Sequences 1, 2 and TST–EHST of 3. Elevated Si/Al and Ti/Al ratios in organic-rich facies were related to apparent eolian (and/or volcanic) input of silica into system. Absence of $CaCO_3$, including pelagic styliolinids, points to possible acidic conditions associated with anoxia and exclusion of carbonate within the depositional system.
2. Shallowing to intermediate depths; basinward progradation of micrite/calcisilt and pelagic deposition of styliolinid carbonate facies on distal, cratonward ramp of foreland basin resulted in high $CaCO_3$ concentrations (EHST–LHST of Sequence 3). Intermediate levels of bioturbation and decreasing TOC/redox-related deposition indicates generally dysoxic conditions.
3. Continued shallowing. Progradation brought fine-grained aluminosilicates across basin trough onto distal ramp. Thin carbonates, dominantly comprised of macroskeletal debris accumulated during transgressive intervals of siliciclastic starvation. Eventual formation of Taghanic Unconformity late in Acadian Tectophase II (Sequences 4 and 5).
4. A second major pulse of deepening, again through a combination of tectonically driven subsidence and eustatic sea level rise (Acadian Tectophase III). Deposition of relatively TOC-rich sediments alternated with more $CaCO_3$-rich sedimentation (Sequence 6).
5. Decline in carbonate deposition under intermediate TOC/redox/oxygenation conditions, indicative of cratonward migration of distal ramp and passing of basinal trough into position of Genesee River Valley. Continued fluctuations of sea level are recorded in Sequences 7 and 8. Wide fluctuations in Si/Al ratio near top of Akzo core indicate introduction of sands during migration of toe of delta platform into Genesee River Valley.

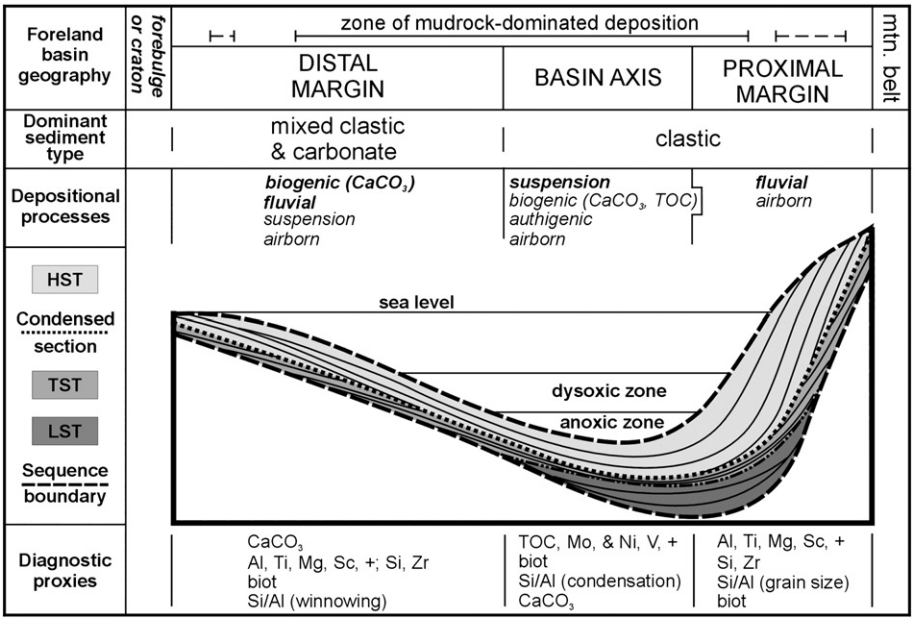

Fig. 10. Foreland basin configuration, sequence stratigraphy and mudrock proxies. Model of proxy utility in mudrock-dominated facies across a foreland basin transect.

6. TOC-rich base of Sequence 9 succeeded by deposition of thick, monotonous EHST succession of gray and black shales. Eventual rise of Si/Al ratio indicates migration of sand-rich facies into western New York during LHST. TOC/redox-related proxies decline to near zero concentrations. Bioturbation indices rise then drop to nothing, apparently associated with high sedimentation rates that swamp benthic burrowing organisms. This interval represents the most significant shallowing event following formation of the Taghanic Unconformity. Progradation of thick wedge of relatively shallow-water sandstone facies indicates migration of proximal delta slope and shelf into position of Cattaraugus Creek Valley.
7. Transgression and short return to anoxic conditions at the position of the Lower Kellwasser extinction event. Black Pipe Creek Shale succeeded by gray, relatively oxygenated and slightly calcareous mudstones with $CaCO_3$ concretions (Sequence 10). Minor progradation of sand-rich facies occurred in the LHST to LST if Sequence 10.
8. Significant transgressive event at position of Upper Kellwasser extinction horizon. Initial high TOC/redox-related sedimentation was followed by a return to gray shales. Rising Si/Al ratio in uppermost samples analyzed in West Valley core appear to presage additional LST sands in apparent upper part of Sequence 11.

Acknowledgements

The authors wish to thank D. Hollander for assistance and insights, and A. Murphy and J. Werne for sharing data on the Geneseo and Oatka Creek formations. The work benefited from Devonian-related discussions with J. Over, G. Baird, W. Kirchgasser, and R. Nyahay, and from geochemistry discussions with T. Lyons, and A. Lermann. A. Murphy assisted with core description, and S. Meyers with statistical analyses. G. Bourgon, M. Fortwengler, and D. Bookwalter assisted in the laboratory. The Akzo Nobel Salt Company, of Retsof, NY generously donated half of Akzo core #9455, and the New York State Geological Survey provided loan of the West Valley core. The project was supported in part by National Science Foundation Grant # EAR-97-25441. Research by Ver Straeten was in part funded by the Northwestern University Environmental Research Council. The manuscript benefited from critical reviews by editor E. Schindler and reviewers D.J. Over and B.J. Witzke.

Appendix A. Supplementary data

Supplementary data to this article can be found online at doi:10.1016/j.palaeo.2010.10.010.

References

Algeo, T.J., Schwark, L., Hower, J.C., 2004. High-resolution geochemistry and sequence stratigraphy of the Hushpuckney Shale (Swope Formation, eastern Kansas): implications for climato-environmental dynamics of the Late Pennsylvanian Midcontinent Seaway. Chemical Geology 206, 259–288.

Arthur, M.A., Sageman, B.B., 2004. Sea-level control on source-rock development: perspectives from the Holocene Black Sea, the Mid-Cretaceous Western Interior Basin on North America, and the Late Devonian Appalachian Basin. In: Harris, N.B. (Ed.), The Deposition of Organic-Carbon-Rich Sediments: Models, Mechanisms, and Consequences: SEPM Special Publication, 82, pp. 35–59.

Baird, G.C., Brett, C.E., Ver Straeten, C.A., 2000. Facies and fossils of the lower Hamilton Group (Middle Devonian) in the Livingston County–Onondaga County region. New York State Geological Association, 72nd Annual Meeting, Field Trip Guidebook, pp. 155–175.

Bandel, K., 1974. Deep-water limestones from the Devonian–Carboniferous of the Carnic Alps, Austria. In: Hsü, K.J., Jenkyns, H.C. (Eds.), Pelagic Sediments on Land and Under the Sea: Special Publication of the International Association of Sedimentologists, 1, pp. 93–116.

Bloch, J., 1998. Shale diagenesis: a currently muddied view. In: Schieber, J., Zimmerle, W., Sethi, P.S. (Eds.), Shales and Mudstones, Volume I. E. Schweizerbart'sche Verlagsbuchhandlung (Nägele u. Obermiller), Stuttgart, pp. 96–106.

Bohacs, K.M., 1998. Contrasting expressions of depositional sequences in mudrocks from marine to non-marine environs. In: Schieber, J., Zimmerle, W., Sethi, P.S. (Eds.), Shales and Mudstones, Volume I. E. Schweizerbart'sche Verlagsbuchhandlung (Nägele u. Obermiller), Stuttgart, pp. 33–78.

Brett, C.E., 1995. Sequence stratigraphy, biostratigraphy, and taphonomy in shallow marine environments. Palaios 10, 597–616.

Brett, C.E., 1998. Sequence stratigraphy, paleoecology, and evolution: biotic clues and responses to sea-level fluctuations. Palaios 13, 241–262.

Brett, C.E., Baird, G.C., 1986. Symmetrical and upward shallowing cycles in the Middle Devonian of New York State and their implications for the punctuated aggradational cycle hypothesis. Paleoceanography 1, 431–445.

Brett, C.E., Baird, G.C., 1990. Submarine erosion and condensation in a foreland basin: examples from the Devonian of Erie County, New York. New York State Geological Association, 62nd Annual Meeting, Field Trip Guidebook, pp. Sun. A1–Sun. A56.

Brett, C.E., Baird, G.C., 1994. Depositional sequences, cycles, and foreland basin dynamics in the late Middle Devonian (Givetian) of the Genesee Valley and western Finger Lakes Region. In: Brett, C.E., Scatterday, J. (Eds.), New York State Geological Association, 66th Annual Meeting, Field Trip Guidebook, pp. 505–586.

Brett, C.E., Baird, G.C., 1996. Middle Devonian sedimentary cycles and sequences in the northern Appalachian basin. In: Witzke, B.J., Ludvigson, G., Day, J.E. (Eds.), Paleozoic Sequence Stratigraphy: Geological Society of America Special Paper, 306, pp. 213–242.

Brett, C.E., Baird, G.C., 2003. Taghanic Stage shelf and off shelf deposits in New York and Pennsylvania: faunal incursions, eustasy, and tectonics. Courier Forschungsinstitut Senckenberg 242, 141–156.

Brett, C.E., Ver Straeten, C.A., 1994. Stratigraphy and facies relationships of the Eifelian Onondaga Limestone (Middle Devonian), in western and west central New York State. In: Brett, C.E., Scatterday, J. (Eds.), New York State Geological Association, 66th Annual Meeting, Field Trip Guidebook, pp. 221–269.

Brett, C.E., Ver Straeten, C.A. (Eds.), 1997. Devonian cyclicity and sequence stratigraphy in New York State. Subcommission on Devonian Stratigraphy (International Union of Geological Sciences Commission on Stratigraphy), Field Trip Guidebook for Amadeus Grabau Symposium, University of Rochester. 369 pp.

Brett, C.E., Miller, K.B., Baird, G.C., 1990. A temporal hierarchy of paleobiologic processes within a Middle Devonian epeiric sea. In: Miller III, W. (Ed.), Paleocommunity Temporal Dynamics: The Long-Term Development of Multispecies Assemblies: The Paleontological Society, Special Publication, 5, pp. 178–209.

Brett, C.E., Baird, G.C., Straeten, Ver, 1997. Middle Devonian (latest Eifelian–Givetian) cycles, sequences, and bio-events in the north-central Appalachian basin. International Meeting on Cyclicity and Bioevents in the Devonian System, Program and Abstracts, Subcommission on Devonian Stratigraphy, p. 21.

Brett, C.E., Baird, G.C., Bartholomew, A.J., DeSantis, M.K., Ver Straeten, C.A., 2011. Sequence stratigraphy and a revised sea-level curve for the Middle Devonian of eastern North America. Palaeogeography, Palaeoclimatology, Palaeoecology. 304, 21–53 (this issue).

Buggisch, W., 1991. The global Frasnian–Famennian "Kellwasser Event.". Geologische Rundschau 80, 49–72.

Calvert, S.E., Pedersen, T.F., 1996. Sedimentary geochemistry of manganese; implications for the environment of formation of manganiferous black shales. Economic Geology 91, 36–47.

Catuneanu, O., 2002. Sequence stratigraphy of clastic systems: concepts, merits, and pitfalls. Journal of African Earth Science 35, 1–43.

Catuneanu, O., Abreu, V., Bhattacharya, J.P., Blum, M.D., Dalrymple, R.W., Eriksson, P.G., Fielding, C.R., Fisher, W.L., Galloway, W.E., Gibling, M.R., Giles, K.A., Holbrook, J.M., Jordan, R., Kendall, C.G., St, C., Macurda, B., Martinsen, O.J., Miall, A.D., Neal, J.E., Nummedal, D., Pomar, L., Posamentier, H.W., Pratt, B.R., Sarg, J.F., Shanley, K.W., Steel, R.J., Strasser, R.J., Tucker, M.E., Winker, C., 2009. Toward the standardization of sequence stratigraphy. Earth Science Reviews 92, 1–33.

Coe, A.L. (Ed.), 2003. The Sedimentary Record of Sea-level Change. Cambridge University Press, New York. 287 pp.

Colton, G.W., de Witt Jr., 1958. Stratigraphy of the Sonyea Formation of Late Devonian age in western and east central New York. U.S. Geological Survey, Oil and Gas Investigations Chart TOC-54.

Creaney, S., Passey, Q.R., 1993. Recurring patterns of total organic carbon and source rock quality within a sequence stratigraphic framework. American Association of Petroleum Geologists Bulletin 77, 386–401.

Cuomo, M.C., Rhoads, D.C., 1987. Biogenic sedimentary fabrics associated with pioneering polychaete assemblages: modern and ancient. Journal of Sedimentary Petrology 57, 537–543.

Curiale, J.A., Cole, R.D., Witmer, R.J., 1991. Application of organic geochemistry to sequence stratigraphic analysis: Four Corners Platform Area, New Mexico, U.S.A. Organic Geochemistry 19, 53–75.

Day, J.E., 1998. Distribution of latest Givetian–Frasnian *Atrypida* (Brachiopoda) in central and western North America. Acta Palaeontologica Polonica 43, 205–240.

Day, J., Uyeno, T.C., Norris, A.W., Witzke, B.J., Bunker, B.J., 1996. Middle–Upper Devonian relative sea-level histories of North American cratonic interior basins. In: Witzke, B.J., Ludvigson, G.A., Day, J. (Eds.), Paleozoic Sequence Stratigraphy, Views from the North American Craton: Geological Society of America Special Paper 306, pp. 259–276.

de Witt Jr., W., Colton, G.W., 1959. Revised correlations of lower Upper Devonian rocks in western and central New York. American Association of Petroleum Geologists Bulletin 43, 2810–2828.

de Witt Jr., W., Colton, G.W., 1978. Physical stratigraphy of the Genesee Formation (Devonian) in western and central New York. U.S. Geological Survey, Professional Paper, 1032-A.

Dean, W.E., Arthur, M.A., 1998. Geochemical expressions of cyclicity in Cretaceous pelagic limestone sequences: Niobrara Formation, Western Interior Seaway. In: Dean, W.E., Arthur, M.A. (Eds.), Stratigraphy and Paleoenvironments of the Cretaceous Western Interior Seaway USA: Society of Economic Paleontologists and Mineralogists, Concepts in Sedimentology and Paleontology, 6, pp. 227–255.

Dennison, J.M., Head, J.W., 1975. Sea level variations interpreted from the Appalachian Basin Silurian and Devonian. American Journal of Science 275, 1089–1120.
Dennison, J.M., Textoris, D.A., 1970. Devonian Tioga tuff in northeastern United States. Bulletin Volcanologique 34, 289–294.
Droser, M.L., Bottjer, D.J., 1986. A semiquantitative field classification of ichnofabric. Journal of Sedimentary Petrology 56, 233–236.
Emerson, S.R., Huested, S.S., 1991. Ocean anoxia and the concentrations of molybdenum and vanadium in seawater. Marine Chemistry 34, 177–196.
Emery, D., Myers, K.J., 1996. Sequence Stratigraphy. Blackwell Science Ltd, Cambridge, MA. 297 pp.
Engleman, E.E., Jackson, L.L., Norton, D.R., 1985. Determination of carbonate carbon in geological materials by coulometric titration. Chemical Geology 53, 125–128.
Ettensohn, F.R., 1985. The Catskill Delta complex and the Acadian Orogeny: a model. In: Woodrow, D.L., Sevon, W.D. (Eds.), The Catskill Delta: Geological Society of America, Special Paper, 201, pp. 39–49.
Filer, J.K., 1994. High frequency eustatic and siliciclastic sedimentation cycles in a foreland basin, Upper Devonian, Appalachian Basin. In: Dennison, J.M., Ettensohn, F.R. (Eds.), Tectonic and Eustatic controls on Sedimentary Cycles: SEPM (Society for Sedimentary Geology), Concepts in Sedimentology and Paleontology, 4, pp. 133–145.
Friedman, G.M., Johnson, K.G., 1966. The Devonian Catskill deltaic complex of New York, type example of a "tectonic delta complex". In: Shirley, M.L., Ragsdale, J.A. (Eds.), Deltas in Their Geologic Framework. Houston Geological Society, pp. 171–188.
Ghibaudo, G., Grandesso, P., Massari, F., Uchman, A., 1996. Use of trace fossils in delineating sequence stratigraphic surfaces (Tertiary Venetian Basin, northeastern Italy). Palaeogeography, Palaeoclimatology, Palaeoecology 120, 261–279.
Goddard, E.N., Trask, P.D., De Ford, R.K., Rove, O.N., Singewald Jr., J.T., Overbeck, R.M., 1948 (reprinted 1984)). Rock Color Chart. Geological Society of America.
Gray, L.M., 1991. Paleoecology, origin, and significance of a shell-rich bed in the lowermost part of the Ludlowville Formation (Middle Devonian, central New York). In: Landing, E., Brett, C.E. (Eds.), Dynamic Stratigraphy and Depositional Environments of the Hamilton Group (Middle Devonian) in New York State, Part II: New York State Museum Bulletin, 469, pp. 93–106.
Griffing, D.H., Ver Straeten, C.A., 1991. Stratigraphy and depositional environments of the lower part of the Marcellus Formation (Middle Devonian) in eastern New York State. In: Ebert, J.R. (Ed.), New York State Geological Association, 63rd Annual Meeting, Field Trip Guidebook, pp. 205–249.
Hallam, A., Bradshaw, M.J., 1979. Bituminous shales and oolitic ironstones as indicators of transgressions and regressions. Journal of the Geological Society of London 136, 157–164.
Hallock, P., Schlager, W., 1986. Nutrient excess and the demise of coral reefs and carbonate platforms. Palaios 1, 389–398.
Hosterman, J.W., 1993. Illite crystallinity as an indicator of the thermal maturity of Devonian black shales in the Appalachian Basin. In: Roen, J.B., Kepferle, R.C. (Eds.), Petroleum Geology of the Devonian and Mississippian Black Shale of Eastern North America: U.S. Geological Survey Bulletin, 1909, pp. G1–G9.
Hosterman, J.W., Whitlow, S.I., 1981. Clay mineralogy of Devonian shales in the Appalachian Basin. U.S. Geological Survey Open-file Report, 81-585.
Hosterman, J.W., Whitlow, S.I., 1983. Clay mineralogy of Devonian shales in the Appalachian Basin. U.S. Geological Survey Professional Paper, 1298. 31 pp.
House, M.R., 1978. Devonian ammonoids from the Appalachians and their bearing on international zonation and correlation. Special Papers In Palaeontology, 21. 70 pp.
House, M.R., Kirchgasser, W.T., 1993. Devonian goniatite biostratigraphy and timing of facies movements in the Frasnian of eastern North America. In: Hailwood, E.A., Kidd, R.B. (Eds.), High Resolution Stratigraphy: Geological Society Special Publication, 70, pp. 267–292.
House, M.R., Kirchgasser, W.T., 2008. Late Devonian goniatites (Cephalopoda, Ammonoidea) from New York State. Bulletins of American Paleontology 374 288 pp.
Isaacson, P.E., Grader, G.W., Diaz-Martinez, E., 1997. Late Devonian (Famennian) glaciation in Gondwana and forced marine regression in North America. Abstracts with Programs, Geological Society of America, 29 (6), p. 117.
Jaminski, J., Algeo, T.J., Maynard, J.B., Hower, J.C., 1998. Climatic origin of dm-scale compositional cyclicity in the Cleveland Member of the Ohio Shale (Upper Devonian), central Appalachian Basin, U.S.A. In: Schieber, J., Zimmerle, W., Sethi, P.S. (Eds.), Shales and Mudstones, Volume I. E. Schweizerbart'sche Verlagsbuchhandlung (Nägele u. Obermiller), Stuttgart, pp. 217–242.
Joachimski, M.M., Breisig, S., Buggisch, W., Mawson, R., Gereke, M., Morrow, J.R., Day, J., Weddige, K., 2009. Devonian climate and reef evolution: insights from oxygen isotopes in apatite. Earth and Planetary Science Letters 284, 599–609.
Johnson, J.G., Klapper, G., Sandberg, C.A., 1985. Devonian eustatic fluctuations in Euramerica. Geological Society of America Bulletin 96, 567–587.
Johnson, J.G., Klapper, G., Elrick, M., 1995. Devonian transgressive–regressive cycles and biostratigraphy, Northern Antelope Range, Nevada. Establishment of reference horizons for global cycles. Palaios 11, 3–14.
Jones, B., Manning, D.A.C., 1994. Comparison of geochemical indices used for the interpretation of palaeoredox conditions in ancient mudstones. Chemical Geology 111, 111–129.
Katz, B.J., Pratt, L.M., 1993. Source rocks in a sequence stratigraphic framework. American Association of Petroleum Geologists, Studies in Geology 37 247 pp.
Kaufmann, B., 2006. Calibrating the Devonian time scale: a synthesis of U–Pb ID-TIMS ages and conodont stratigraphy. Earth Science Reviews 76, 175–190.
Kirchgasser, W.T., Baird, G.C., Brett, C.E., 1989. Regional placement of Middle/Upper Devonian (Givetian–Frasnian) boundary in western New York State. In: McMillan, N.H., Embry, A.F., Glass, D.H. (Eds.), Devonian of the World: Canadian Society of Petroleum Geologists, Memoir, 14 (3), pp. 113–117.
Kirchgasser, W.T., Over, D.J., Woodrow, D.L., 1994. Frasnian (Upper Devonian) strata of the Genesee River Valley, western New York State. In: Brett, C.E., Scatterday, J. (Eds.), New York State Geological Association, 66th Annual Meeting, Field Trip Guidebook, pp. 325–358.
Klapper, G., 1971. Sequence within the conodont genus *Polygnathus* in the New York lower Middle Devonian. Geologica et Palaeontologica 5, 59–79.
Klapper, G., 1981. Review of New York Devonian conodont biostratigraphy. In: Oliver Jr., W.A., Klapper, G. (Eds.), Devonian Biostratigraphy of New York, Part 1: International Union of Geological Sciences, Subcommission on Devonian Stratigraphy, pp. 57–66.
Klapper, G., 1989. The Montagne Noire Frasnian (Upper Devonian) conodont succession. In: McMillan, N.H., Embry, A.F., Glass, D.H. (Eds.), Devonian of the World: Canadian Society of Petroleum Geologists, Memoir, 14 (3), pp. 449–478.
Klapper, G., Kirchgasser, W.T., Baesemann, J.F., 1995. Graphic correlation of a composite standard for the Frasnian (Upper Devonian). In: Mann, K.O., Lane, H.R. (Eds.), Graphic Correlation: SEPM Special Publication, 53, pp. 177–184.
Lichte, F.E., Golightly, D.W., Lamothe, P.J., 1987. Inductively coupled plasma-atomic emission spectrometry. In: Baedecker, P.A. (Ed.), Methods for Geochemical Analysis: U.S. Geological Survey Bulletin, 1770, pp. B1–B10.
Macquaker, J.H.S., Taylor, K.G., 1996. A sequence stratigraphic interpretation of a mudstone-dominated succession: the Lower Jurassic Cleveland ironstone Formation, U.K. Journal of the Geological Society of London 153, 759–770.
Macquaker, J.H.S., Gawthorpe, R.L., Taylor, K.G., Oates, M.J., 1998. Heterogeneity, stacking patterns, and sequence stratigraphic interpretation in distal mudstone successions: examples from the Kimmeridge Clay Formation, U.K. In: Schieber, J., Zimmerle, W., Sethi, P.S. (Eds.), Shales and Mudstones, Volume I. E. Schweizerbart'sche Verlagsbuchhandlung (Nägele u. Obermiller), Stuttgart, pp. 163–186.
Mann, U., Stein, R., 1997. Organic facies variations, source rock potential, and sea level changes in Cretaceous black shales of the Quebrada Ocal, upper Magdalena Valley, Columbia. American Association of Petroleum Geologists Bulletin 81, 556–576.
Mayer, S.M., 1994. Field studies of the Middle Devonian Ludlowville–Moscow sequence in the Genesee and Seneca Valleys, New York State. In: Brett, C.E., Scatterday, J. (Eds.), New York State Geological Association, 66th Annual Meeting, Field Trip Guidebook, pp. 491–503.
Mayer, S.M., Baird, G.C., Brett, C.E., 1994. Correlation of facies divisions in the uppermost Ludlowville Formation (Givetian) across western and central New York State. In: Landing, E. (Ed.), Studies in Stratigraphy and Paleontology in Honor of Donald W. Fisher: New York State Museum Bulletin, 481, pp. 229–264.
McCollum, L.B., 1991. Revised stratigraphy, sedimentology, and paleoecology of the Ledyard Member, Ludlowville Formation, New York. In: Landing, E., Brett, C.E. (Eds.), Dynamic Stratigraphy and Depositional Environments of the Hamilton Group (Middle Devonian) in New York State, Part II: New York State Museum Bulletin, 469, pp. 107–128.
Miall, A.D., 1991. Stratigraphic sequences and their chronostratigraphic correlation. Journal of Sedimentary Petrology 61, 497–505.
Miller, K.B., 1991. High-resolution correlation within a storm-dominated muddy epeiric sea: Taphofacies of the Middle Devonian Wanakah Member, western New York. In: Landing, E., Brett, C.E. (Eds.), Dynamic Stratigraphy and Depositional Environments of the Hamilton Group (Middle Devonian) in New York State, Part II: New York State Museum Bulletin, 469, pp. 129–152.
Murphy, A.E., Sageman, B.B., Hollander, D.J., Straeten, Ver, 2000a. Organic carbon burial and faunal dynamics in the Appalachian basin during the Devonian (Givetian–Famennian) greenhouse: an integrated paleoecological/biogeochemical approach. In: Huber, B., MacLeod, K., Wing, S. (Eds.), Warm Climates in Earth History. Cambridge University Press, pp. 351–385.
Murphy, A.E., Sageman, B.B., Hollander, D.J., Lyons, T.W., Brett, C.E., 2000b. Black shale deposition and faunal overturn in the Devonian Appalachian basin: clastic starvation, seasonal water-column mixing, and efficient biolimiting nutrient recycling. Paleoceanography 15, 280–291.
Murphy, A.E., Sageman, B.B., Hollander, 2000c. Eutrophication by decoupling of the marine biogeochemical cycles of C, N, and P: a mechanism for the Late Devonian mass extinction. Geology 28, 427–430.
Ormiston, A.R., Oglesby, R.J., 1995. Effect of Late Devonian paleoclimate on source rock quality and location. In: Huc, A.-Y. (Ed.), Paleogeography, Paleoclimate, and Source Rocks: American Association of Petroleum Geologists, Studies in Geology, 40, pp. 105–133.
Over, D.J., Hopkins, T.L., Obligado, A., Rotondo, K.A., Spaziani, A.L., Warner, N., 2001. Sequences in Upper Devonian black shales of the Appalachian Basin: Middlesex, Rhinestreet, and the Frasnian–Famennian boundary interval. Geological Society of America, Abstracts with Programs 33 (1), p. 17.
Pasley, M.A., Gregory, W.A., Hart, G.F., 1991. Organic matter variations in transgressive and regressive shales. Organic Geochemistry 17, 483–509.
Payton, C.E., 1977. Seismic stratigraphy — applications to hydrocarbon exploration. American Association of Petroleum Geologists, Memoir 26.
Pepper, J.F., de Witt Jr., W., 1950. Stratigraphy of the Upper Devonian Wiscoy Sandstone and equivalent Hanover Shale in western and central New York. U.S. Geological Survey, Oil and Gas Investigations, Chart TOC 37.
Pepper, J.F., de Witt Jr., W., Colton, G.W., 1956. Stratigraphy of the West Falls Formation of Late Devonian age in western and central New York. U.S. Geological Survey, Oil and Gas Investigations, Chart TOC 55.
Posamentier, H.W., Allen, G.P., 1999. Siliciclastic sequence stratigraphy — concepts and applications. SEPM (Society for Sedimentary Geology), Concepts in Sedimentology and Paleontology 7 210 pp.
Potter, P.E., Maynard, J.B., Pryor, W.A., 1980. Sedimentology of Shale. Springer Verlag, New York. 306 pp.
Potter, P.E., Maynard, J.B., Depetris, P.J., 2005. Mud and Mudstones. Springer, New York. 297 pp.

Rast, N., Skehan, J.W., 1993. Mid-Paleozoic orogenesis in the North Atlantic. In: Roy, D.C., Skehan, J.W. (Eds.), The Acadian Orogeny: Recent Studies in New England, maritime Canada, and the Autochthonous Foreland: Geological Society of America Special Paper, 275, pp. 153–164.
Reaves, C.M., 1986. Organic matter metabolizability and calcium carbonate dissolution in nearshore marine muds. Journal of Sedimentary Petrology 56, 486–494.
Rickard, L.V., 1975. Correlation of the Silurian and Devonian rocks in New York State. New York State Museum, Map And Chart No. 24.
Roen, J.B., Kepferle, R.C., 1993. Petroleum geology of the Devonian and Mississippian black shale of Eastern North America. U.S. Geological Survey Bulletin 1909 Chapters A–N.
Sageman, B.B., 1996. Lowstand tempestites: depositional model for Cretaceous skeletal limestones, Western Interior Basin. Geology 24, 888–892.
Sageman, B.B., Lyons, T.W., 2003. Geochemistry of fine-grained sediments and sedimentary rocks. In: MacKenzie, F. (Ed.), Treatise on Geochemistry, 7. Elsevier Publishing, pp. 115–158.
Sageman, B.B., Murphy, Werne, J.P., Ver Straeten, C.A., Hollander, D.J., Lyons, T.W., 2003. A tale of shales: the relative roles of production, decomposition, and dilution in the accumulation of organic-rich strata, Middle–Upper Devonian, Appalachian basin. Chemical Geology 195, 229–273.
Savrda, C.E., 1991. Ichnology in sequence stratigraphic studies: an example from the Lower Paleocene of Alabama. Palaios 6, 39–53.
Schieber, J., 1998. Developing a sequence stratigraphic framework for the Late Devonian Chattanooga Shale of the southeastern US: relevance for the Bakken Shales. In: Christopher, J.E., Gilboy, C.F., Paterson, D.F., Bend, S.L. (Eds.), Eighth International Williston Basin Symposium: Saskatchewan Geological Society, Special Publication, 13, pp. 58–68.
Schieber, J., 1999. Distribution and deposition of mudstone facies in the Upper Devonian Sonyea Group of New York. Journal of Sedimentary Research 69, 909–925.
Schieber, J., Zimmerle, W., 1998. Introduction and overview: the history and promise of shale research. In: Schieber, J., Zimmerle, W., Sethi, P.S. (Eds.), Shales and Mudstones, Volume I. E. Schweizerbart'sche Verlagsbuchhandlung (Nägele u. Obermiller), Stuttgart, pp. 1–10.
Schieber, J., Zimmerle, W., Sethi, P.S., 1998. Shales and Mudstones, Volumes I and II. E. Schweizerbart'sche Verlagsbuchhandlung (Nägele u. Obermiller), Stuttgart.
Schlager, W., 1992. Sedimentology and sequence stratigraphy of reefs and carbonate platforms. American Association of Petroleum Geologists, Continuing Education Course Notes Series, 34. 71 pp.
Schutter, S.R., 1998. Characteristics of shale deposition in relation to stratigraphic sequence systems tracts. In: Schieber, J., Zimmerle, W., Sethi, P.S. (Eds.), Shales and Mudstones, Volume I. E. Schweizerbart'sche Verlagsbuchhandlung (Nägele u. Obermiller), Stuttgart, pp. 79–108.
Schwalbach, J.R., Bohacs, K.M., 1992. Sequence stratigraphy in fine-grained rocks: examples from the Monterey Formation. Pacific Section, SEPM, Field Trip Guide, 70. 55 pp.
Scotese, C.R., McKerrow, W.S., 1990. Revised world maps and introduction. In: McKerrow, W.S., Scotese, C.R. (Eds.), Palaeozoic Palaeogeography and Biogeography: Memoir, Geological Society of London, 12, pp. 1–21.
Sethi, P.S., Leithold, E.L., 1997. Recurrent depletion of benthic oxygen with 4th-order transgressive maxima in the Cretaceous Western Interior Seaway. Palaeogeography, Palaeoclimatology, Palaeoecology 128, 39–61.
Shaw, D.M., 1954. Trace elements in pelitic rocks, part I: variation during metamorphism. Bulletin of the Geological Society of America 65, 1151–1166.
Sloss, L.L., 1963. Sequences in the cratonic interior of North America. Geological Society of America Bulletin 74, 93–114.
Spencer, D.W., Degens, E.T., Kulbicki, G., 1967. Factors affecting element distributions in sediments. In: Ahrens, L.H. (Ed.), Origin and Distribution of the Elements. Pergamon Press, New York, pp. 981–998.
Tribovillard, N., Algeo, T.J., Lyons, T., Riboulleau, A., 2006. Trace metals as paleoredox and paleoproductivity proxies. An update. Chemical Geology 232, 12–32.
Tucker, M.E., 1974. Sedimentology of Paleozoic pelagic limestones: the Devonian Griotte (southern France) and Cephalopodenkalk (Germany). In: Hsü, K.J., Jenkyns, H.C. (Eds.), Pelagic Sediments on Land and Under the Sea: Special Publication of the International Association of Sedimentologists, 1, pp. 71–92.
Tucker, R.D., Bradley, D.C., Ver Straeten, C.A., Harris, A.G., Ebert, J.R., McCutcheon, S.R., 1998. New U–Pb zircon ages and the duration and division of Devonian time. Earth and Planetary Science Letters 158, 175–186.
Vail, R.R., Mitchum Jr., R.M., Todd, R.G., Widmier, J.M., Thompson III, S., Sangree, J.B., Bubb, J.N., Hatleid, W.G., 1977. Seismic stratigraphy and global changes in sea level. In: Payton, C.E. (Ed.), Seismic Stratigraphy — Applications to Hydrocarbon Exploration: American Association of Petroleum Geologists, Memoir, 26, pp. 49–62.
Van Wagoner, J.C., Posamentier, H.W., Mitchum, R.M., Vail, P.R., Sarg, K.G., Loutit, T.S., Hardenbol, J., 1988. An overview of the fundamentals of sequence stratigraphy and key definitions. In: Wilgus, C.K., Hastings, B.S., Kendall, C.G.St.C., Posamentier, H.W., Ross, C.A., Van Wagoner, H.C. (Eds.), Sea-Level Changes: An Integrated Approach: Society of Economic Paleontologists and Mineralogists, Special Publications, 42, pp. 39–45.
van Wagoner, J.C., Mitchum, R.M., Campion, K.M., Rahmanian, V.D., 1990. Siliciclastic sequence stratigraphy in well logs, cores, and outcrop: concepts for high resolution correlation of time and facies. American Association of Petroleum Geologists, Methods in Exploration Series, 7. 55 pp.
Ver Straeten, C.A., 1994. Microstratigraphy and depositional environments of a Middle Devonian foreland basin: Berne and Otsego members, Mount Marion Formation, eastern New York State. In: Landing, E. (Ed.), Studies in Stratigraphy and Paleontology in Honor of Donald W. Fisher: New York State Museum Bulletin, 481, pp. 367–380.
Ver Straeten, C.A., 1996. Stratigraphic synthesis and tectonic and sequence stratigraphic framework, upper Lower and Middle Devonian, Northern and Central Appalachian Basin. Unpublished Ph.D. dissertation, University of Rochester.
Ver Straeten, C.A., 2004. K-bentonites, volcanic ash preservation, and implications for Lower to Middle Devonian volcanism in the Acadian Orogen, Eastern North America. Geological Society of America Bulletin 116, 474–489.
Ver Straeten, C.A., 2007. Basinwide stratigraphic synthesis and sequence stratigraphy, Upper Pragian, Emsian and Eifelian stages (Lower to Middle Devonian), Appalachian Basin. In: Becker, R.T., Kirchgasser, W.T. (Eds.), Devonian Events and Correlations: Geological Society of London, Special Publications, 278, pp. 39–81.
Ver Straeten, C.A., Brett, C.E., 1995. Lower and Middle Devonian foreland basin fill in the Catskill Front: stratigraphic synthesis, sequence stratigraphy, and the Acadian Orogeny. In: Garver, J.I., Smith, J.A. (Eds.), New York State Geological Association, 67th Annual Meeting, Field Trip Guidebook, pp. 313–356.
Ver Straeten, C.A., Griffing, D.H., Brett, C.E., 1994. The lower part of the Middle Devonian Marcellus "Shale", central to western New York State: stratigraphy and depositional history. In: Brett, C.E., Scatterday, J. (Eds.), New York State Geological Association, 66th Annual Meeting, Field Trip Guidebook, pp. 271–321.
Vogel, K., Golubic, S., Brett, C.E., 1987. Endolith associations and their relation to facies distribution in the Middle Devonian of New York State, U.S.A. Lethaia 20, 263–290.
Wendt, J., Aigner, T., 1985. Facies patterns and depositional environments of Paleozoic cephalopod limestones. Sedimentary Geology 44, 263–300.
Werne, J.P., Sageman, B.B., Lyons, T.W., Hollander, D.J., 2002. An integrated assessment of a "type euxinic" deposit: evidence for multiple controls on black shale deposition in the Middle Devonian Oatka Creek Formation. American Journal of Science 302, 110–143.
Wignall, P.B., 1991a. Test of the concepts of sequence stratigraphy in the Kimmeridgian of England and northern France. Marine Petroleum Geology 8, 430–441.
Wignall, P.B., 1991b. Model for transgressive black shales? Geology 19, 167–170.
Wignall, P.B., Maynard, J.R., 1993. The sequence stratigraphy of transgressive black shales. In: Katz, B.H., Pratt, L.M. (Eds.), Source Rocks in a Sequence Stratigraphic Framework: American Association of Petroleum Geologists, Studies in Geology, 37, pp. 35–47.
Wilgus, C.K., Hastings, B.S., Kendall, C.G.St.C., Posamentier, H.W., Ross, C.A., Van Wagoner, 1988. Sea-level changes: an integrated approach. SEPM Special Publication, No. 42. 407 pp.
Williams, C.J., Hesselbo, S.P., Jenkyns, H.C., Morgans-Bell, H.S., 2001. Quartz silt in mudrocks as a key to sequence stratigraphy (Kimmeridge Clay Formation, Late Jurassic, Wessex Basin, UK). Terra Nova 13, 449–455.
Wintsch, R.P., Kvale, C.M., 1994. Differential mobility of elements in burial diagenesis of siliciclastic rocks. Journal of Sedimentary Research A64, 349–361.
Witzke, B.J., 1990. Palaeoclimatic constraints for Palaeozoic palaeolatitudes of Laurentia and Euramerica. In: McKerrow, W.S., Scotese, C.R. (Eds.), Palaeozoic Palaeogeography and Biogeography: Memoir, Geological Society of London, 12, pp. 57–73.
Woodrow, D.L., Sevon, W.D., 1985. The Catskill Delta. Geological Society of America Special Paper, No. 201. 246 pp.
Young, G.M., Nesbitt, H.W., 1998. Processes controlling the distribution of Ti and Al in weathering profiles, siliciclastic sediments and sedimentary rocks. Journal of Sedimentary Research 68, 448–455.